

A MULTI-EPOCH STUDY OF THE RADIO CONTINUUM EMISSION OF ORION SOURCE I: CONSTRAINTS ON THE DISK EVOLUTION OF A MASSIVE YSO AND THE DYNAMICAL HISTORY OF ORION BN/KL

C. GODDI, E. M. L. HUMPHREYS

European Southern Observatory, Karl-Schwarzschild-Strasse 2, D-85748 Garching bei München and
Harvard-Smithsonian Center for Astrophysics, 60 Garden Street, Cambridge, MA 02138

L. J. GREENHILL

Harvard-Smithsonian Center for Astrophysics, 60 Garden Street, Cambridge, MA 02138

AND

C. J. CHANDLER

National Radio Astronomy Observatory, P.O. Box O, Socorro, NM 87801

AND

L. D. MATTHEWS

MIT Haystack Observatory, Westford, MA 01886

Draft version November 16, 2021

ABSTRACT

We present new $\lambda 7$ mm continuum observations of Orion BN/KL with the Very Large Array (VLA). We resolve the emission from the Young Stellar Objects (YSO) radio Source I and BN at several epochs. Radio Source I is highly elongated northwest-southeast, and remarkably stable in flux density, position angle, and overall morphology over nearly a decade. This favors the extended emission component arising from an ionized edge-on disk rather than an outwardly propagating jet.

We have measured the proper motions of Source I and BN for the first time at 43 GHz. We confirm that both sources are moving at high speed (12 and 26 km s⁻¹, respectively) approximately in opposite directions, as previously inferred from measurements at lower frequencies. We discuss dynamical scenarios that can explain the large motions of both BN and Source I and the presence of disks around both. Our new measurements support the hypothesis that a close (~ 50 AU) dynamical interaction occurred around 500 years ago between Source I and BN as proposed by Gomez et al. From the dynamics of encounter we argue that Source I today is likely to be a binary with a total mass on the order of 20 M_⊙, and that it probably existed as a softer binary before the close encounter. This enables preservation of the original accretion disk, though truncated to its present radius of ~ 50 AU.

N-body numerical simulations show that the dynamical interaction between a binary of 20 M_⊙ total mass (Source I) and a single star of 10 M_⊙ mass (BN) may lead to the ejection of both and binary hardening. The gravitational energy released in the process would be large enough to power the wide-angle, high-velocity flow traced by H₂ and CO emission in the BN/KL nebula. Assuming the proposed dynamical history is correct, the smaller mass for Source I recently estimated from SiO maser dynamics ($\gtrsim 7$ M_⊙) by Matthews et al., suggests that non-gravitational forces (e.g. magnetic) must play an important role in the circumstellar gas dynamics.

Subject headings: ISM: individual objects: Orion BN/KL - stars: formation - (stars:) binaries (including multiple): close - methods: N-body simulations

1. INTRODUCTION

The Orion BN/KL complex, at a distance of 418 ± 6 pc (Menten et al. 2007; Kim et al. 2008), contains the nearest region of ongoing high-mass star formation. A dense protostellar cluster lies within the region containing three radio sources that are believed to be massive young stellar objects (YSOs): the highly embedded radio Source I, (Greenhill et al. 2004a; Reid et al. 2007; Matthews et al. 2010); the BN object, which is the brightest source in the region in the mid-infrared (IR) at 12.4 μ m (Gezari et al. 1998); and Source *n*, a relatively evolved YSO with a disk observed in the MIR (Greenhill et al. 2004b) and a jet observed in the radio at 8.4 GHz (Menten & Reid 1995; Gómez et al. 2008).

Despite intensive investigations at radio and IR wavelengths, the primary heating source(s) for the Orion KL

region ($L \sim 10^5 L_{\odot}$) is (are) still not known. Another long-standing puzzle is the geometry of outflow and the identification of driving sources. There are two large-scale outflows in the region. A powerful (3×10^{47} ergs), high-velocity (30–200 km s⁻¹), wide-angle (~ 1 rad) outflow extends northwest-southeast (NW-SE) over 0.3 pc. This so-called “high-velocity” outflow is traced in CO emission (Chernin & Wright 1996; Zapata et al. 2009) and in 2.12 μ m H₂ shocked emission originating in finger-like structures that end in bow shocks (Allen & Burton 1993). A second, “low-velocity” outflow (~ 18 km s⁻¹) is identified by a cluster of bright $v = 0$ SiO and H₂O masers, concentrated within a few arcsec around Source I and elongated northeast-southwest (NE-SW; Genzel & Stutzki 1989; Greenhill et al. 1998, and in prep.).

Source I has been proposed as a possible driver of

both the high-velocity NW-SE outflow (e.g., Wright et al. 1995; Greenhill et al. 1998; Bally & Zinnecker 2005) and the low-velocity NE-SW outflow (Beuther et al. 2005; Greenhill et al. 2004a and in prep.). Confusion arises because the radio continuum emission from Source I shows an elongated structure, which has been interpreted as both an ionized jet along a NW-SE direction (Bally & Zinnecker 2005; Tan 2008a) and as an ionized disk with a NE-SW spin axis (Reid et al. 2007).

Based on a multi-epoch observational campaign of several SiO maser transitions using the Very Large Array (VLA) and the Very Long Baseline Array (VLBA), Matthews et al. (2010) and Greenhill et al. (in prep.) provide convincing evidence that Source I is associated with a disk/outflow system with a NE-SW axis. In particular, based on a VLBA monitoring of $v = 1, 2$ $J = 1-0$ SiO maser transitions, Matthews et al. (2010) presented a movie of bulk gas flow tracing a compact disk and the base of a protostellar outflow at radii < 100 AU from Source I. In addition, Greenhill et al. measured proper motions of $v = 0$ SiO masers, which trace the bipolar outflow expanding with a characteristic velocity ~ 18 km s $^{-1}$ and extending to radii of 100-1000 AU from Source I along a NE-SW axis, parallel to the axis of the disk/outflow system traced by $v = 1, 2$ masers at radii < 100 AU.

The origin and nature of the wide-angle NW-SE oriented outflow, traced in shocked H $_2$ and CO emission, is still a matter of debate. Rodríguez et al. (2005) proposed that Source I and BN had a close encounter about 500 yrs ago, which resulted in the ejection of interacting sources and the formation of a tight binary (Source I). Based on a proper motion study of radio sources at 8.4 GHz, Gómez et al. (2008) proposed that Source I, BN, and source n participated in the same dynamical interaction 500 yrs ago and that all three sources are moving away from the putative center of interaction. The energy liberated in the process may provide in principle sufficient energy to power the fast NW-SE outflow (Bally & Zinnecker 2005; Zapata et al. 2009). It is not clear, however, what effect a close passage and consequent formation of a tight binary would have on a well-organized accretion/outflow structure such as observed in Source I (Matthews et al. 2010). Tan (2004, 2008b) proposed an alternatively scenario where a close passage between Source I and BN (a runaway star from the Trapezium) would trigger a tidally-enhanced accretion and subsequent outburst of outflow activity, resulting in the powerful high-velocity outflow.

In this paper, we present new multi-epoch, high-angular resolution observations of the radio continuum emission in Orion BN/KL at 7 mm (43 GHz) from the VLA. The main goals of the new observations were to investigate the nature of the radio continuum in Source I and reconstruct the dynamical history of BN/KL. In particular, we investigate changes in morphology, size, and flux density as a function of time (over a decade) and frequency (43 vs 8.4 GHz) to obtain insights into the nature of the radio sources, mainly to test the ionized disk and jet hypotheses proposed for Source I. In addition, we measured absolute proper motions of radio sources based on accurate absolute astrometry, with the aim of constraining the dynamical history of the BN/KL region. In order to quantify probabilities of different dynamical

scenarios, we present also new N-body simulations of decaying protostellar clusters with a varying number of objects. Previous N-body simulations for BN/KL (Gómez et al. 2008) assumed a five-member cluster having large masses (in the range 8-20 M $_{\odot}$), which resulted in the formation of binaries with total mass of 36 M $_{\odot}$. However, there is no evidence of such massive objects in the BN/KL region, based on present data. Our new simulations assume more plausible masses of individual objects as well as investigate a larger number of possible scenarios.

The current paper is structured as follows. The observational setup and data calibration procedures are described in § 2. § 3 reports the results of the multi-epoch study. In § 4, we discuss the morphological evolution of the radio continuum from Source I and its interpretation in terms of an ionized disk. In § 5 we suggest that Source I and BN had a past close passage, based on proper motion measurements. In § 6, we discuss dynamical scenarios that can explain the origin of the proper motions measured for Source I and BN. § 7 and 8 discuss problems related to the mass of Source I and a possible origin for the fast, wide-angle H $_2$ outflow, respectively. Finally, conclusions are drawn in § 9.

2. OBSERVATIONS AND DATA REDUCTION

Observations of the $\lambda 7$ mm continuum emission in Orion BN/KL were made using the Very Large Array (VLA) of the National Radio Astronomy Observatory (NRAO)¹. We present data obtained in four distinct epochs spanning over 8 years (see Table 1). All data were obtained while the VLA was in the A-configuration, yielding a resolution of approximately 0''05².

In order to image the continuum emission from radio sources in BN/KL and to provide a strong signal as a phase-reference to calibrate the phase and amplitude of the (weak) continuum signal, we employed a dual-band continuum setup with a narrow band (6.25 MHz in programs AC952 and AC817; 3.25 MHz in AG622; and 1.56 MHz in AM668A), centered on the SiO $v = 1, J = 1-0$ line (rest frequency 43122 MHz), and a broad band (50 MHz) centered on a line-free portion of the spectrum (offset in frequency from the maser by: ~ 350 MHz for AC952, ~ 100 MHz for AC817 and AG622, ~ 40 MHz for AM668). Both frequency bands were observed in dual-circular polarizations. Absolute flux density calibration was obtained from observations of 3C286 or 3C48 (depending on the epoch). Short (60 s) scans of the nearby (1.3 $^{\circ}$) QSO J0541-0541 (measured flux density in the range 0.7-1.5 Jy, depending on the epoch) were alternated with 60 s scans of Source I to monitor amplitude gains, tropospheric and instrumental phase variations, and to determine the electronic phase offsets between the bands.³ We then self-calibrated the narrow-band $v = 1$ SiO maser data, applied the derived phase and amplitude corrections to the broadband continuum data, and

¹ NRAO is a facility of the National Science Foundation operated under cooperative agreement by Associated Universities, Inc.

² Project AM668A was conducted in A configuration plus the Pie Town VLBA antenna.

³ In AM668A, the QSO 0501-019 was observed every 25 minutes (relatively infrequently compared with the timescale of tropospheric and instrumental phase variations), so no absolute astrometry was available for that program.

TABLE 1
 PARAMETERS OF OBSERVATIONS.

Program	Date	T^a (h)	Synthesized Beam ($R = 0$) ^b $\theta_M(\prime\prime) \times \theta_m(\prime\prime); P.A.(^\circ)$	RMS (mJy/bm)	Synthesized Beam ($R = 8$) ^b $\theta_M(\prime\prime) \times \theta_m(\prime\prime); P.A.(^\circ)$	RMS (mJy/bm)
AM668A ^c	2000/11/10	6.6	$0.041 \times 0.028; -30$	0.14	$0.058 \times 0.045; -20$	0.13
AG622 ^d	2002/03/31	2.7	$0.046 \times 0.034; -4$	0.16	$0.066 \times 0.047; -17$	0.14
AC817	2006/04/15	0.9	$0.051 \times 0.030; 11$	0.28	$0.066 \times 0.044; -5$	0.24
AC952	2009/01/12	3.3	$0.058 \times 0.039; 3$	0.11	$0.079 \times 0.053; +4$	0.11

NOTE. —

^aApproximate on-source integration time.

^bSynthesized beams correspond to images made using the AIPS task IMAGR with a robust parameter $R = 0$ and $R = 8$, respectively.

^cArchival data from the program AM668A have been published by Reid et al. (2007).

^dData from the program AG622 have been published by Rodríguez et al. (2005).

 TABLE 2
 PARAMETERS OF THE 7 MM SOURCES IN ORION BN/KL

Sources	α (J2000) (^h ^m ^s)	δ (J2000) ([°] ['] ^{''})	e_t e_n e_s e_ν (mas)	Flux Density (mJy)	Angular Size $\theta_M(\prime\prime) \times \theta_m(\prime\prime); P.A.(^\circ)$
BN	05 35 14.1094	-05 22 22.724	5 0.3 1 \lesssim 2	23 ± 2	$0.095 \pm 0.007 \times 0.072 \pm 0.008; 38 \pm 10$
I	05 35 14.5141	-05 22 30.575	5 1 1 \lesssim 2	11 ± 2	$0.23 \pm 0.01 \times 0.12 \pm 0.01; 142 \pm 2$
n	05 35 14.3571	-05 22 32.719	5 4 0 \lesssim 2	1.2 ± 0.1	$0.126 \pm 0.018 \times 0.064 \pm 0.01; 6 \pm 8$
H	05 35 14.5008	-05 22 38.691	5 2 0 \lesssim 2	1.3 ± 0.1	$0.075 \pm 0.015 \times 0.053 \pm 0.01; 4 \pm 8$

 NOTE. — The source names refer to Lonsdale et al. (1982), Garay et al. (1987), and Churchwell et al. (1987). The positions, flux densities, and sizes reported here are from the January 12 2009 epoch. Angular sizes were derived as described in the Text. The quoted uncertainties represent the dispersion among images with various weighting schemes. Individual contributions to the total error budget (~ 5 mas) on absolute positions are listed: e_t , e_n , e_s , e_ν (see Appendix).

produced a high-quality map of the continuum emission. A detailed description of this calibration procedure can be found in Goddi et al. (2009).

Using the Astronomical Image Processing System (AIPS) task IMAGR, we made images of the BN/KL region with 4096×4096 pixels and cell size $0''.005$ to cover a $20''$ field. We produced maps with two different weightings of the (u,v) data, first setting the IMAGR “ROBUST” weighting parameter to $R = 8$ (equivalent to natural weighting) and then to $R=0$. We restored these image with a circular beams with FWHM 59 mas and 47 mas, respectively. The sizes of these restoring beams are approximately the average of the geometric-mean sizes among different epochs (see Table 1). Since the synthesized beam size in the AC952 program was larger ($\sim 20\%$) than that in other programs, this choice resulted in a degradation of the resolution for other epochs. For this reason, we also produced images with round restoring beams of 40 mas ($R = 0$ weighting) and 50 mas ($R = 8$ weighting), equal to the geometric-mean size of the beams in projects AC817 and AG622, thus slightly “super-resolving” AC952. The “high-resolution” maps were used to analyze structural changes in the continuum emission from Source I (Sect. 4), whilst the “low-resolution” images were used to fit positions and track proper motions of the continuum sources in BN/KL (Sect. 5), since they minimize structural effects in locating the peak of emission.

3. RESULTS

Four continuum sources were detected above a 6σ lower limit of ~ 0.1 mJy beam $^{-1}$ in the most sensitive epoch (2009 January 12): BN, I, n , H (Lonsdale et al. 1982; Garay et al. 1987; Churchwell et al. 1987). For each de-

tected source, a two-dimensional ellipsoidal Gaussian model was fitted in a 100×100 pixel area around the peak emission, using the AIPS task JMFIT. For Source I, we used the AIPS task OMFIT to directly fit the visibilities using a disk model geometry, which is more appropriate for the elongated morphology of the emission than the Gaussian model fitted by JMFIT (see below). The positions, flux densities, and deconvolved angular sizes of the detected sources for the 2009 January 12 epoch are given in Table 2. The flux densities obtained for BN and Source I are in good agreement with the values previously reported in the literature (Menten & Reid 1995; Reid et al. 2007). source n was recently detected with the VLA for the first time at 7 mm by Rodríguez et al. (2009), who reports a flux density of 2 ± 0.2 mJy. This a factor ~ 2 higher than what we found in 2009 January 12. The discrepancy might be due either to a different filtering of the total flux in the two observations ($0''.05$ vs $0''.2$ beam) or to intrinsic variability of source n , possibly due to non-thermal nature of the continuum emission (Menten & Reid 1995). Based on a comparison between 7 mm and 3.6 cm observations, however, Rodríguez et al. (2009) estimated a spectral index of 0.2 for the continuum emission from source n , suggestive of marginally thick free-free thermal emission, as expected in an ionized outflow. Since the 3.6 cm emission is extended over $0''.6$ (i.e., an order of magnitude more than the restoring beam in A-configuration), the variation in flux between measurements with different angular resolutions is most probably due to filtering of the total flux in the most extended configuration.

Our images of the continuum emission from Source I at 43 GHz for the 2009 January 12 epoch are shown in Figure 1, where different weightings and restoring beams

were used (59 mas, top panel; 47 mas, middle panel). The emission is composed of a compact component at the center and a component elongated NW-SE. In order to better demonstrate the structure of the elongated component, we have subtracted a 6 mJy (beam-sized) Gaussian component at the centroid of the emission. The resulting image (Fig. 1, bottom panel) reveals a structure with a radius of ~ 45 AU and a brightness of about $4.5 \text{ mJy beam}^{-1}$, elongated at a position angle (P.A.) of $142 \pm 2^\circ$. It is barely resolved along the minor axis and has a deconvolved axial ratio of about 2:1. The radius of this elongated structure agrees to within uncertainties with previous measurements reported by Reid et al. (2007). Rodríguez et al. (2009) report a smaller size for Source I at 7 mm ($0''.09 \pm 0''.01 \times 0''.06 \pm 0''.02$). Their image, however, has lower sensitivity than the ones reported here, owing to shorter integration time and narrow bandwidth employed (line-free channels were used to map the continuum), hence the quoted size refers to the central compact component while the elongated component is not detected.

Figure 2 shows a comparison among images of Source I at different epochs. Both size and position angle of the continuum emission appear to be remarkably constant over the last decade.

Extreme care was used in computing the absolute astrometry for the three new (non-archival) datasets reported here, the accuracy of which we quantify as ~ 5 mas (see Appendix). This accurate absolute astrometry enabled us to track proper motions for BN and Source I over three epochs. Figure 3 shows the contour images of BN and Source I at different epochs. The displacement of the peaks in each image shows the absolute proper motions of the radio continuum emission for both sources. The consistency of morphology in the continuum emission at different epochs reinforces the robustness of the motion measurements. The proper motions have been calculated by performing an error-weighted linear least-squares fit of positions with time (Figure 4). The uncertainties of the absolute proper motions are the formal errors of the linear least-squares fits and depend mainly on the error of the absolute position of individual sources at different epochs. The derived absolute proper motions and associated uncertainties are reported in Table 3. The measured proper motions are in the range $15\text{--}22 \text{ km s}^{-1}$, confirming the large proper motions of sources I and BN found previously at 8.4 GHz by Gómez et al. (2008). In Table 3, we also report the absolute proper motions of both sources in the Orion Nebular Cluster (ONC) rest-frame and relative proper motion of BN with respect to Source I. The ONC rest-frame is obtained by subtracting the mean absolute proper motions of 35 radio sources located within a radius of 0.1 pc from the core of the ONC, $\mu_\alpha \cos \delta = +0.8 \pm 0.2 \text{ mas yr}^{-1}$; $\mu_\delta = -2.3 \pm 0.2 \text{ mas yr}^{-1}$, $\text{PA} = 341 \pm 5^\circ$ (Gómez et al. 2005).

Based on only two epochs, source *n* and H do not show significant proper motions in right ascension or declination at a typical 3σ upper limit of $3\text{--}4 \text{ mas yr}^{-1}$.

4. MORPHOLOGICAL EVOLUTION OF THE RADIO CONTINUUM: AN IONIZED DISK AROUND SOURCE I

The continuum emission from Source I shows an elongated structure with a position angle of $142^\circ \pm 3^\circ$ and a size ~ 45 AU (Fig. 1). The uncertainty quoted here

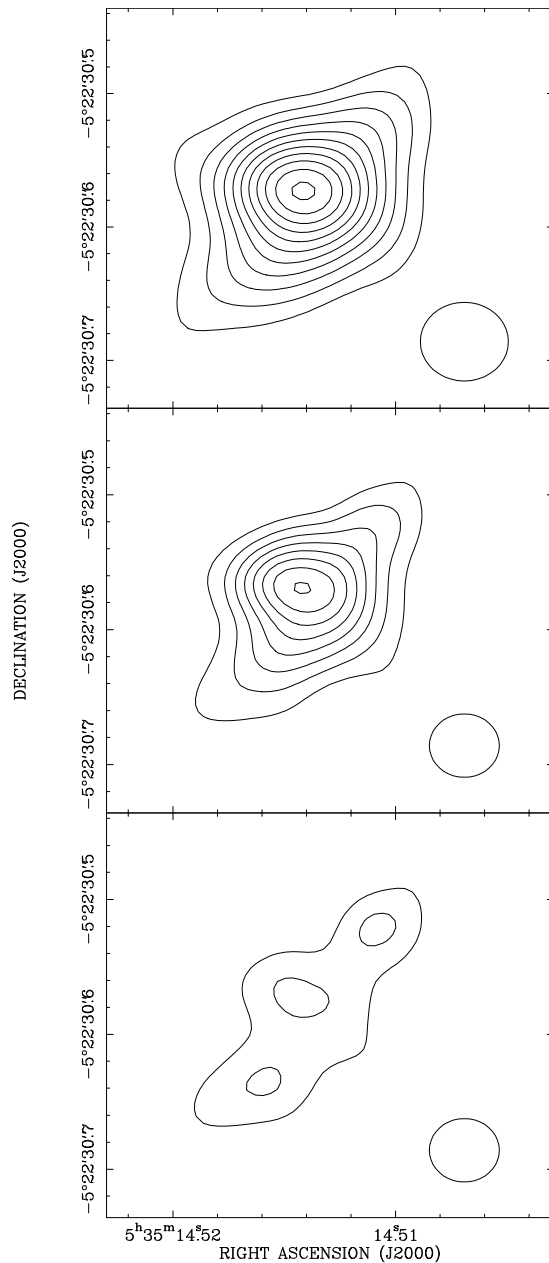


FIG. 1.— Continuum images of Source I in Orion BN/KL at 43 GHz made with the VLA in the A configuration (2009 January 12). The images have been produced with natural weighting and a round restoring beam of 59 mas (*upper panel*) and with a $R = 0$ weighting and a round restoring beam of 47 mas (*middle and lower panel*), respectively. In order to demonstrate the elongated structure, we subtracted a (6 mJy, 50 mas size) Gaussian component at the centroid of the emission (*lower panel*). In all images the contour levels are at integer multiples of $0.4 \text{ mJy beam}^{-1}$. The FWHM of the restoring beams are shown in the bottom right corner of each panel. We interpret the northwest-southeast elongated emission, as coming from an ionized disk surrounding Source I (see also Reid et al. 2007).

for the position angle represents the dispersion of values measured in several epochs, which is not significantly larger than the uncertainty in a single epoch (2°) reported in Table 2. A comparison among images at different epochs does not show any evidence of changes in structure, size or position angle over 8 years (Fig. 2). In addition, we found no evidence for significant variations

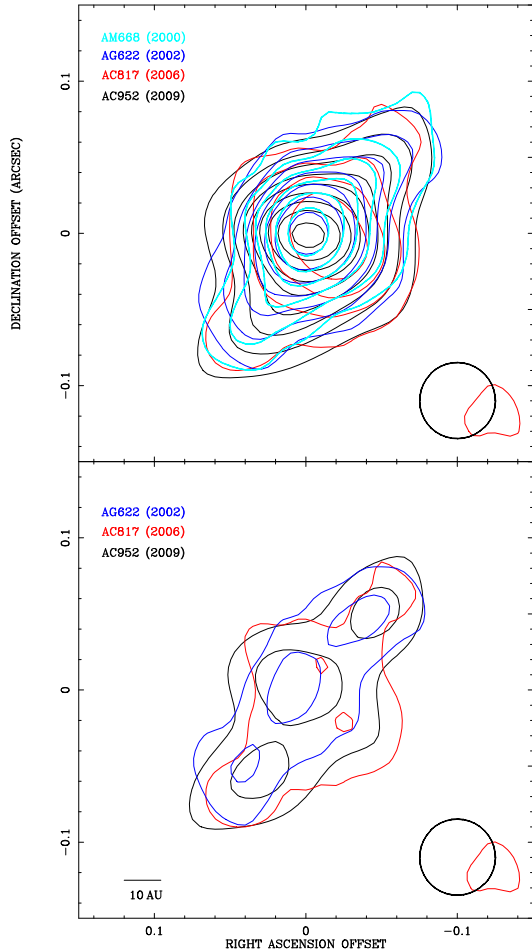


FIG. 2.— Continuum images of Source I in Orion BN/KL at 43 GHz observed with the VLA in the A configuration at several epochs (*upper panel*). We subtracted the brightest component near the center in each epoch (*lower panel*). The images have been produced with natural weighting and a circular restoring beam of 50 mas (*bottom right corner*). The contour levels are at integer multiples of 0.4 mJy beam⁻¹ (2000), 0.5 mJy beam⁻¹ (2002), 0.7 mJy beam⁻¹ (2006), 0.4 mJy beam⁻¹ (2009). The choice of contours is dictated by differing sensitivity and uv-coverage in different experiments (Table 1). There is no significant change in the morphology or position angle of the structure over ~ 8 years ($142^\circ \pm 2^\circ$).

in the total 7 mm continuum flux density of Source I over the last decade, with all values being consistent with 11 ± 2 mJy.

What is the nature of this ionized emission? The centimeter-to-millimeter wavelength spectrum of the entire source can be characterized as a power law with flux density $S_\nu \propto \nu^{1.6}$ (Beuther et al. 2006). The emission is optically thick up to 100 GHz, with a dust component dominating above 300 GHz (Beuther et al. 2006). The radio emission has been interpreted either as an ionized jet with a NW-SE axis (Bally & Zinnecker 2005; Tan 2008a) or as an ionized disk with a NE-SW axis (Reid et al. 2007). In the following, we will discuss three alternative interpretations of the radio continuum emission from Source I: 1) an ionized jet, 2) an equatorial wind, and 3) an accreting disk. We will show that only the latter is consistent with our multi-epoch data.

If the emission originates in an ionized jet, one would expect to detect structural variations owing to motions

of individual jet components. In fact, when observed with high-angular resolution, radio jets do not show a smooth structure, but contain clumps. Using multi-epoch VLA observations, detection of proper motions as large as ~ 100 -500 km s⁻¹ have been reported in the components of radio continuum jets associated with both low-mass YSOs (e.g., HH1-2 -Rodríguez et al. 2000) and high-mass YSOs (e.g., Cepheus-A - Curiel et al. 2006; HH80-81 - Marti et al. 1995). Assuming 20 km s⁻¹ as a lower limit for the expansion velocity of the jet associated with Source I (as estimated from the SiO maser flow by Matthews et al. 2010), displacements of ~ 40 AU are expected on a temporal baseline of 9 years. Such displacements are comparable to the radius of the continuum emission and are easily detectable with the linear resolution of our observations (~ 25 AU). In principle, no structural changes would be expected from an optically thin, homogeneous ionized region. However, even in the case of uniform density, thermal pressure would drive expansion of the ionized region as a whole, as seen for ionized winds and HII regions (e.g., Acord et al. 1998). As well, classic models of spherical winds (Panagia & Felli 1975) and ionized jets (Reynolds 1986) predict the size of the ionized region to vary as a function of frequency as $\nu^{-0.7}$, which would imply a factor of 3 change in size between 8.4 GHz and 43 GHz. Nonetheless, deconvolved sizes obtained for the radio continuum emission around Source I are similar at the two frequencies: $0''.23 \times 0''.115$ at 43 GHz (this work) and $0''.19 \times <0''.15$ at 8.4 GHz (Gómez et al. 2008).

An alternative interpretation is that the radio emission from Source I arises in a disk-like structure rather than in a jet, where the gas is not accreting but rather consists of an equatorial ionized wind. Such an equatorial wind has been modeled by Drew et al. (1998). The model predicts that the radiation pressure (mediated by line opacity) from a massive YSO accelerates material from the surface of the disk and blows it away mainly in the equatorial plane. The velocities obtained for the gas are of the order of a few hundreds km s⁻¹. Also in this scenario, large changes in morphology are expected over short time intervals (i.e., a few years) owing to fast motions of clumps in the wind, as observed in the luminous YSO S140 IRS1 (Hoare 2006). In addition to fast motions, rapid changes in the wind structure are expected as well, owing to small changes in illumination by the ionizing YSO and to the inherently unstable nature of the radiation-driven winds (Owocki et al. 1988). Hence, we conclude that our multi-epoch data are not consistent with the picture of a radiation-driven disk-wind model.

Finally, we consider the case that the elongated structure traces ionized accreting gas in a disk. Keto (2003) has shown that, even when the inner portion of a disk is fully ionized, accretion of (ionized and neutral) material can continue onto a massive YSO. In this spherically symmetric model, the gravitational attraction of the star exceeds the outward force of the (radiation and thermal) pressure inside a critical radius $r_c = GM/2c_s$, where G is the gravitational constant, M is the mass of the YSO, and c_s is the sound speed in the ionized material. In the hypothesis of spherical accretion, by scaling the stellar parameters in Table 1 from Keto (2003) to a 10 M_⊙ star, ionized accretion can proceed inside of the critical radius ~ 25 AU with an accretion rate $\sim 10^{-5}$ M_⊙ yr⁻¹.

This critical radius is reasonably consistent with the disk size observed at 43 GHz in Source I. In Sect. 6, we report evidence for Source I being a binary of total mass of the order of $20 M_{\odot}$. In the most probable case of an equal-mass binary, this would slightly increase the critical radius above, estimated in the assumption of one $10 M_{\odot}$ single star. We note that similar values for the critical radius and accretion rates are obtained for models of ionized accretion in the presence of significant angular momentum (Keto 2007), as required by the disk geometry in Source I. We also note that an accretion rate of $10^{-5} M_{\odot} \text{ yr}^{-1}$ and a central stellar mass of 10 to $20 M_{\odot}$ is consistent with a luminosity of a few times $10^4 L_{\odot}$ for Source I.

The interpretation of the ionized elongated structure as a disk versus a jet is relevant to a key longstanding question regarding Orion BN/KL: what are the drivers of the region's outflows? In our interpretation, the elongated radio continuum structure traces a nearly edge-on disk, with a spin axis aligned NE-SW, parallel to the low-velocity outflow (see § 1). This is consistent with the model for Source I based on high-resolution monitoring of several SiO maser transitions (Kim et al. 2008; Matthews et al. 2010; Greenhill et al. 2004a and in prep). Greenhill et al. (in prep.) estimated a *mass-loss rate* of the NE-SW outflow to be $3 \times 10^{-6} M_{\odot} \text{ yr}^{-1}$, assuming a gas density of 10^6 cm^{-3} (required for the excitation of $v = 0$ SiO masers), a typical velocity of 18 km s^{-1} for the outflow, and a radius of 100 AU. Based on the models of Keto (2007), we estimate an *accretion rate* $\sim 10^{-5} M_{\odot} \text{ yr}^{-1}$. A ratio of O(0.1) for the mass-loss rate to the accretion rate is typical of values inferred from observations of low-mass pre-main-sequence stars (e.g., Bontemps et al. 1996) and of values predicted in MHD ejection models (Shu et al. 2000; Konigl & Pudritz 2000). This might indicate that Source I is still in an active accretion stage. We caution that the mass-loss rate of the outflow from Source I estimated from the SiO masers is accurate only to within an order of magnitude (Greenhill et al., in prep.). Nevertheless, the preponderance of evidence strongly supports a picture where the high-mass YSO Source I is powering a disk/outflow system along a NE-SW axis.

5. PROPER MOTIONS: A CLOSE PASSAGE BETWEEN SOURCE I AND THE BN OBJECT

We observe BN and Source I moving with high speeds in opposite direction with respect to one another. This result confirms previous independent proper motion measurements at 8.4 GHz (Gómez et al. 2008) and at multiple frequencies ranging from 8.4 to 43 GHz (Rodríguez et al. 2005). Figure 5 shows maps of the absolute proper motions of both sources in the ONC rest-frame (upper panel) and relative proper motion of BN with respect to Source I (lower panel).

The more accurate relative proper motions show that Source I falls within the error cone of the BN past motion (Fig. 5, lower panel). Based on our accurate relative astrometry, we can estimate the minimum separation BN and Source I had in the past in the plane of the sky by extrapolating the velocity vector backward in time and assuming no acceleration. Following Gómez et al.

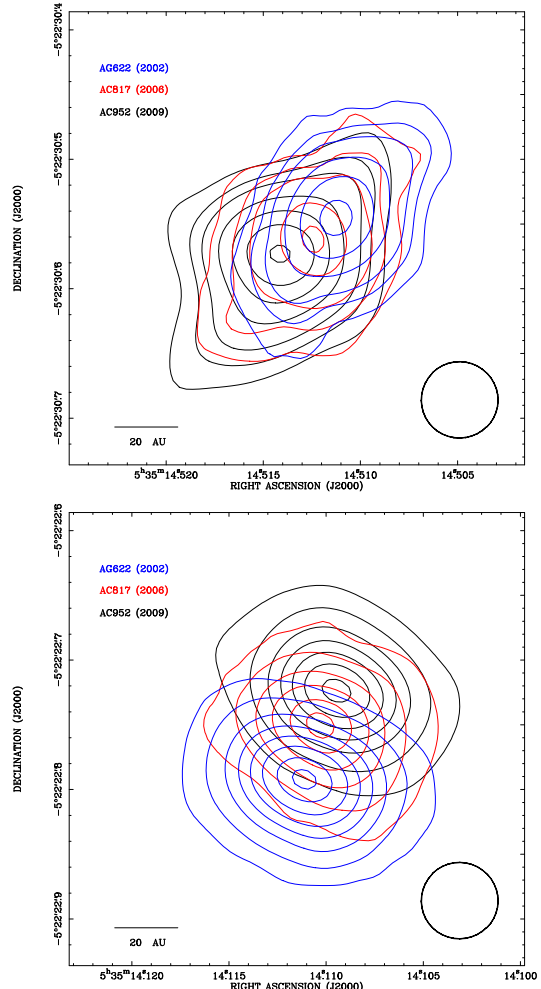


FIG. 3.— Contours for the 2002 (blue), 2006 (red), and 2009 (black) epochs of radio source I (upper panel) and the BN object (lower panel). Contours are $(1, 2, 3, 5, 7, 9, 11) \times 0.5$ (2002), 0.7 (2006) and 0.4 (2009) mJy beam^{-1} (upper panel), and $(1, 3, 6, 9, 12, 15, 18, 20) \times 0.7$ (2002), 0.9 (2006) and 0.7 (2009) mJy beam^{-1} (lower panel). The images have been restored with a circular beam with FWHM 59 mas (bottom right corner). The displacement of the peaks in each image shows the absolute proper motions of the radio continuum emission of Source I and BN. (2008), the minimum separation is

$$S_{\min}(\prime\prime) = \frac{|x_{2002.25}\mu_y - y_{2002.25}\mu_x|}{\sqrt{\mu_x^2 + \mu_y^2}}$$

which occurs at an epoch t_{\min} given by

$$T_{\min}(\text{years}) = 2002.25 - \frac{|x_{2002.25}\mu_x + y_{2002.25}\mu_y|}{\mu_x^2 + \mu_y^2}$$

where both quantities are expressed as a function of the relative position for program AG622 ($x_{2002.25} = -5.974\prime\prime \pm 0.002\prime\prime$, $y_{2002.25} = 7.752\prime\prime \pm 0.002\prime\prime$) and relative proper motions of BN with respect to Source I ($\mu_x = -0.0107\prime\prime \pm 0.0003\prime\prime \text{ yr}^{-1}$, and $\mu_y = 0.0142\prime\prime \pm 0.0003\prime\prime \text{ yr}^{-1}$). By substituting these values, we obtain: $S_{\min} = 0\prime\prime.109 \pm 0\prime\prime.175$ and $T_{\min} = 1453 \pm 9$ years. Hence, our new measurements indicate that, about 560 years ago, BN and Source I were as close as 50 ± 100 AU in projection on the plane of the sky.

TABLE 3
 PROPER MOTIONS OF RADIO SOURCE I AND THE BN OBJECT

Sources	μ_α (mas yr ⁻¹)	μ_δ (mas yr ⁻¹)	μ_{tot} (mas yr ⁻¹)	V_x (km s ⁻¹)	V_y (km s ⁻¹)	V_{mod} (km s ⁻¹)	P.A. (deg)
<i>Absolute proper motions</i>							
I	6.3 ± 1.1	-4.2 ± 1.1	7.6 ± 1.1	12.3 ± 2.1	-8.3 ± 2.1	14.9 ± 2.1	123.9 ± 8.2
BN	-3.5 ± 1.1	10.4 ± 1.1	11.0 ± 1.1	-6.9 ± 2.1	20.4 ± 2.1	21.5 ± 2.1	341.3 ± 5.5
<i>Proper motions relative to I</i>							
BN	-10.7 ± 0.3	14.2 ± 0.3	17.8 ± 0.3	-21.0 ± 0.6	27.9 ± 0.6	34.9 ± 0.6	323.0 ± 1.0
<i>Proper motions in the ONC rest-frame</i>							
I	5.5 ± 1.1	-1.9 ± 1.1	5.8 ± 1.1	10.8 ± 2.1	-3.8 ± 2.2	11.5 ± 2.1	109.4 ± 10.9
BN	-4.3 ± 1.1	12.7 ± 1.1	13.4 ± 1.1	-8.5 ± 2.1	25.0 ± 2.1	26.4 ± 2.1	341.2 ± 4.6

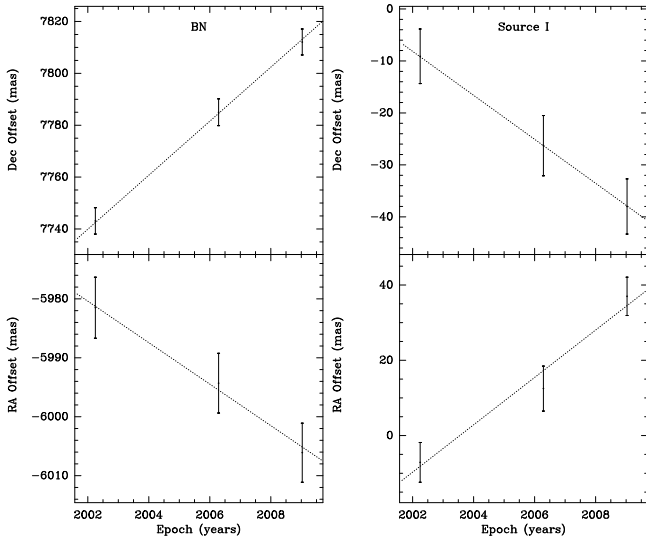


FIG. 4.— Measured absolute proper motions in RA and DEC of the radio continuum centroid of Source I and BN, relative to position $\alpha(J2000) = 05^h 35^m 14^s.5116$, $\delta(J2000) = -05^\circ 22' 30'' 536$. In each panel, the dotted line shows the proper motion calculated by the (variance-weighted) linear least-squares fit of the positional offsets with time.

Although we do not have position information along the line-of-sight that confirms the close passage in 3-dimensions (proper motion analysis gives only a 2-dimension description of the dynamics), the line of sight velocities of BN and Source I are also consistent with a dynamical encounter. Based on the measured radial velocities of the ambient molecular cloud ($V_{\text{LSR}}=9$ km s⁻¹: Genzel & Stutzki 1989), BN ($V_{\text{LSR}}=20$ km s⁻¹, or 11 km s⁻¹ with respect to the ambient cloud: Rodríguez et al. 2009), and Source I ($V_{\text{LSR}}=5$ km s⁻¹, or -4 km s⁻¹ with respect to the ambient cloud: Matthews et al. 2010), the ratio of radial velocities between BN and Source I is ~ 2.7 , which is consistent with the value of 2.3 determined from the (ONC-frame) velocities in the plane of the sky. Hence, 5 to 6 observables are consistent with the hypothesis of a close passage between Source I and BN. We also note that the closest approach separation of 50 AU is comparable to the radius of the ionized disk observed today around Source I (Sect. 4). As this is compact for a high-mass YSO accretion disk, we suggest that it may have been truncated in the close encounter with BN. We note also that the ionized envelope surrounding BN has a comparable radius of ~ 40 AU (Table 2), consistent with the

truncation hypothesis.

Gómez et al. (2008) measured a large proper motion for source n as well ($\mu = 13 \pm 1$ mas yr⁻¹, $v = 25 \pm 2$ km s⁻¹, P.A. = $180^\circ \pm 4^\circ$) using position measurements at 8.4 GHz and proposed a close passage with BN and Source I. This result however disagrees with our measurements. Using two epochs in which we achieved 5 – 6 σ detections at 7 mm wavelength, we measured a much smaller proper motion of 3.7 ± 1.6 mas yr⁻¹ and PA = 26 ± 22 in the ONC rest-frame. This indicates that source n is moving either very slowly or not at all (our measurement is consistent with 0 within $\sim 2\sigma = 3.2$ mas yr⁻¹). In addition, the proper motion vector points towards and not away from the interaction center, as it would be required if source n were truly ejected by a close passage with Source I and BN. As a final point, the proper motion of source n at 8.4 GHz reported by Gómez et al. (2008) should be viewed with a degree of caution. The emission at 8.4 GHz from source n is resolved into a bipolar or elongated structure, depending on epoch (size $\sim 0''.6$), and the systematic error in the motion may arise from internal variability. Tracking of northern and southern components of source n by Gómez et al. (2008) may be possible, but a longer time baseline is required for certainty. Of some concern, the dataset from Gómez et al. (2008) is not homogeneous in terms of observing set-up among epochs, and hence changes in uv-coverage could mimic change in structure/position. Finally, in their Figure 2, Gómez et al. (2008) show that the displacement of source n in the plane of the sky from the cluster origin is approximately half that of BN. However, this is inconsistent with the two objects having comparable proper motions and starting their outward motion from the same point of origin and epoch (assuming linearity and constancy of motion). Further observation of source n is required to confirm the proper motion measured at 8.4 GHz and hence the dynamical interaction with BN and Source I.

In the following section, we will reconstruct the dynamical history of BN/KL based on the proper motions measured for Source I and BN. Section 6.3.2 will discuss the possible dynamical role of source n , in the assumption that the 8.4 GHz proper motion measurement of Source n derived by Gómez et al. (2008) is correct.

6. DYNAMICAL HISTORY OF BN/KL

Observations have increasingly shown that stars are almost never born in isolation but favor formation in clusters, where interactions can occur among members

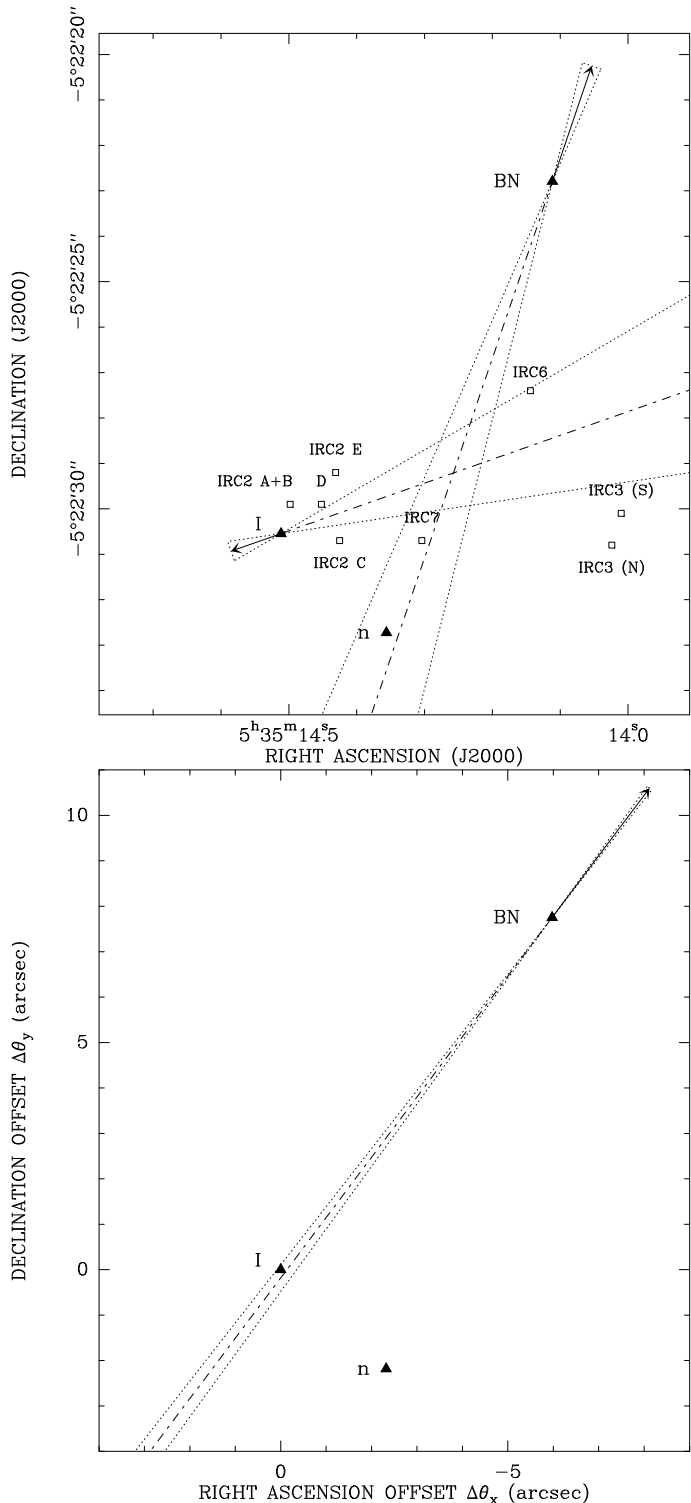


FIG. 5.— Proper motions of BN and Source I measured from our multi-epoch datasets in the ONC rest-frame (*upper panel*). Proper motion of BN relative to Source I (*lower panel*). The arrows indicate proper motion direction and displacement for 200 yr. The dashed lines indicate errors in proper motion position angle, and they track backwards showing past positions of source. About 560 years ago, BN, Source I, and several IR sources within the BN/KL region were located within a few arcseconds of each other. Our measurements are consistent with a null proper motion for source *n*.

of a collapsing protostellar group. Interactions with sibling stars play an even more important role in the formation of high-mass stars (Bally & Zinnecker 2005). YSOs are also surrounded by circumstellar disks and envelopes, which can play a role in this context by increasing the interaction radius among members of the collapsing protostellar cluster (e.g. Moeckel & Bally 2006). The anomalously large relative motions between BN and Source I suggest that interactions have also played an important role in Orion BN/KL. In the following sections, we investigate four scenarios to account for the observed dynamics of the region: 1) the motions are independent and BN is a runaway star from the Trapezium cluster (Sect 6.1); 2) a close passage between the two protostars resulted in a star-disk interaction (Sect 6.2); 3) the motions are the result of a multiple (≥ 3) body interaction within a cluster of individual YSOs, where a tight massive binary is formed (Source I) that carries away the binding energy of the system and BN is ejected (Sect 6.3); 4) a close passage between BN and Source I, a pre-existing massive binary, resulted in the acceleration of both stars and the hardening of the original binary (Sect 6.5).

6.1. Scenario 1: Dynamical ejection of BN from θ^1 Ori C

We consider first the possibility that the motions of BN and Source I are independent. Tan (2004, 2008b) proposed that BN was ejected from the Trapezium by dynamical interaction involving the θ^1 Ori C binary system.

In a triple system usually the lightest member is ejected, sometimes as a runaway star, while an eccentric binary is formed between the remaining stars. The formation of a tight binary is required if the system was originally bound, as a consequence of energy conservation. Usually, both components (star and close binary) leave their parental envelope, with velocities inversely proportional to their masses, as a consequence of momentum conservation (e.g. Reipurth 2000).

θ^1 Ori C seems to have the physical properties predicted for such a dynamical event: an eccentric, massive binary with primary and secondary masses greater than that of BN (Kraus et al. 2007); a total orbital energy ($E_{tot} \sim 3 \times 10^{47}$ erg) greater than the kinetic energy of BN (10^{47} erg); a proper motion roughly in the opposite direction to the motion of BN and with approximately the predicted magnitude (for the dynamical mass of BN). However, our absolute proper motion measurement is inconsistent with a close encounter between BN and θ^1 Ori C in the past. Figure 6 shows the radio-ONC-frame⁴ proper motion of BN, $\mu_x = -4.3 \pm 1.1$ mas yr⁻¹, $\mu_y = +12.7 \pm 1.1$ mas yr⁻¹ (Table 3), and the optical-ONC-frame⁵ proper motion of θ^1 Ori C, $\mu_x = +1.4 \pm 0.17$ mas yr⁻¹; $\mu_y = -1.8 \pm 0.16$ mas yr⁻¹

⁴ The radio-ONC-frame is defined by the mean absolute proper motions of 35 radio sources located within a radius of 0.1 pc from the core of the ONC, $\mu_\alpha \cos \delta = +0.8 \pm 0.2$ mas yr⁻¹; $\mu_\delta = -2.3 \pm 0.2$ mas yr⁻¹, PA=341 \pm 5° (Gómez et al. 2005).

⁵ The optical-ONC-frame is defined by the mean absolute proper motions of 73 stars brighter than $V \sim 12.5$ located within a radius of one-half degree of the Trapezium, corresponding to an average proper motion dispersion of 0.70 ± 0.06 mas yr⁻¹ (van Altena et al. 1988).

(van Altena et al. 1988). The plot shows that past trajectories of BN and θ^1 Ori C in fact intersect far from the Trapezium cluster. By repeating the same analysis we made for the relative motions of BN with respect to Source I (this time referring positions and velocities to θ^1 Ori C⁶), we obtain $x_{BN} = -35.4'' \pm 0.3''$, $y_{BN} = 60.0'' \pm 0.3''$, $\mu_x = -0.0057'' \pm 0.0011'' \text{ yr}^{-1}$, and $\mu_y = 0.0145'' \pm 0.0011'' \text{ yr}^{-1}$ (P.A. = $339 \pm 4^\circ$) for the *relative* proper motions between BN and θ^1 Ori C (today). This yields $S_{\min} = 10.9'' \pm 4.8''$ and $T_{\min} = -2403 \pm 312$ years. Hence, our measurements indicate that probably BN and θ^1 Ori C did not get closer than ~ 5000 AU in the past. This large separation is much greater than the gravitational radius that corresponds to the inferred escape speed of BN, which argues against a close encounter. Nevertheless, the accuracy of our measurement (at a 2.3σ level) does not conclusively exclude it. We note that the uncertainties here are a factor of 5 larger than quoted by Gómez et al. (2008), whose analysis used the relative motion of BN with respect to Source I to achieve a greater accuracy. However, since Source I has a large absolute proper motion (see Table 3), using the BN motion relative to Source I is undesirable.

Apart from the measurements reported in this paper, there is a number of pieces of evidence that are inconsistent with an ejection of BN from θ^1 Ori C. First, θ^1 Ori C and BN have similar absolute radial velocities measured in the ONC rest-frame, -15 km s^{-1} (Stahl et al. 2008) and 11 km s^{-1} (Rodríguez et al. 2009), respectively, which is inconsistent with momentum conservation, since BN is approximately five times less massive than θ^1 Ori C. Second, a close passage of BN and θ^1 Ori C would explain the large proper motion of only BN but not that of Source I. We note that in order to reach a velocity dispersion of 15 km s^{-1} , a stellar cluster on the order of 1000 AU in extent would have to reach $250 M_\odot$, which is greater than the mass concentrations believed to exist in the part of BN/KL local to Source I. Third, this scenario would not explain the close passage ($\sim 0''.1$) of BN with Source I, since it would be a notable coincidence for a high-velocity YSO ejected from a massive binary to pass so close to another high-mass YSO. Finally, BN exhibits characteristics of a star much younger than any of the Trapezium members, which according to Hillenbrand (1997) are a few million years old. While none of the Trapezium stars are surrounded by obvious circumstellar material, BN is surrounded by a molecular disk (Scoville et al. 1983; Beuther et al. 2010) and by a hypercompact HII region with a $\sim 20 \text{ AU}$ radius, implying that this star is dragging along a significant amount ($> 10^{-4} M_\odot$) of dense circumstellar gas (Scoville et al. 1983; Bally & Zinnecker 2005).

6.2. Scenario 2: Two-body interaction: star-disk encounter with BN

We now consider the case where BN and Source I were initially unbound and approached to within $\sim 50 \text{ AU}$ (Sect. 5). Source I is surrounded by an ionized disk, indicating a massive (possibly still accreting) protostar (Sect. 4). A close passage by a massive star (BN) should

⁶ For θ^1 Ori C we took the absolute position from the COUP X-ray survey: $05^{\text{h}}35^{\text{m}}16.4789^{\text{s}}$, $05^\circ 23' 22.844''$, known to an accuracy of $0''.3$ (Getman et al. 2005).

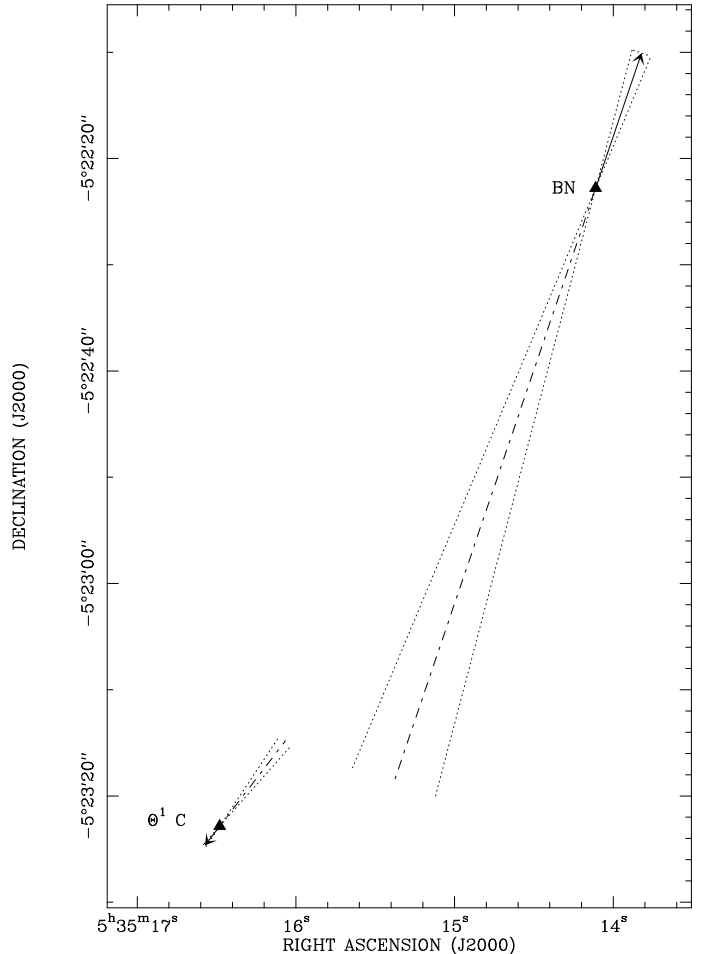


FIG. 6.— Absolute proper motions of BN (radio, this work) and θ^1 Ori C (optical, van Altena et al. 1988) measured in the ONC-rest-frame. The arrows indicate proper motion direction and displacement on the plane of the sky over 1000 years. The dash-dot line indicates motion backward over 4400 years, assuming it is linear. The dashed lines indicate 1σ uncertainties in position angles. The minimum separation on the sky between BN and θ^1 Ori C was $10.9'' \pm 4.8''$.

produce tides in the disk and enhance accretion (e.g. Ostriker 1994). In particular, Pfalzner (2006) has shown that disks around massive YSOs located in clusters can experience angular momentum losses of up to $\sim 50\%$ - 95% (with consequent increases in accretion), as a result of gravitational interaction during stellar encounters; this is termed *cluster-assisted accretion*.

Although star-disk interaction at the center of clusters can affect accretion, it cannot itself lead to stellar ejection. In fact, a two-body interaction does not allow efficient transfer of momentum and/or energy between the two objects. On the contrary, simulations show that disk-assisted capture increases binary formation rates (Moeckel & Bally 2007). In order to account for the large (positive) total energy of the BN-I system, the formation of a tight binary that develops a large negative-binding energy is required, a consequence of momentum and energy conservation.

In conclusion, in order to end up with stellar ejections, the original system must have contained three or more objects, and one of the successor systems must now be a tight binary.

TABLE 4
SUMMARY OF DYNAMICAL SCENARIOS FOR BN/KL AND N-BODY SIMULATION OUTCOMES.

Scenario	M_*^a (M_\odot)	M_{bin}^b (M_\odot)	Ejections ^c (%)	S_{min} Passage ^d (AU)	Sect.
3-body: * * * \Rightarrow * (* *) BN, I (new binary)	10,10,10	10+10	0.1	7	6.3.1
4-body: * * * * \Rightarrow * * (* *) BN, I, n (new binary) ^e	10,10,5,5 10,10,9,1	5+5 9+1	< 0.1 < 0.1	- -	6.3.2 6.3.2
11-body: 11 \times (*) \Rightarrow 9 \times (*) (* *) IRcx,BN,n,I (new binary)	0.5(\times 2),1(\times 2),2(\times 2) 3(\times 1),5(\times 1),10(\times 3)	10+10 10+5	0.2 0.2	5 4	6.3.3 6.3.3
3-body: * (* *) \Rightarrow * (* *) BN(single), I (old binary)	10,10+10	10+10	38	16	6.5

NOTE. —

^aStellar masses in the N-body simulations.

^bMasses of binary components that remain after ejection of stars from the system.

^cFraction of cases leading to the ejection of a massive ($\sim 10 M_\odot$) object.

^dAverage minimum passage (and binary separation) for cases that include an ejection.

^eIt assumes that n is a binary with a 5+5 or 9+1 M_\odot total mass, source I and BN two single $10 M_\odot$ stars.

6.3. Scenario 3: Three and more-body interactions: single stars

In this Section, we describe different scenarios that can result in the high proper motion of multiple stars: a triple system (Sect. 6.3.1), a quadruple system (Sect. 6.3.2), and a stellar cluster (Sect. 6.3.3). In order to test different scenarios and quantify statistical probabilities, we ran N-body simulations using the NBODY0 code from Aarseth (1985).⁷ We numerically integrated several thousand cases of cluster decays with different initial numbers of bodies. Table 4 summarizes the key aspects and likelihood of different scenarios, which will be described in detail in the following subsections. We note that each scenario involves the ejection of individual stars and concomitant formation of a tight binary. The presence of a disk around Source I poses a challenge for some arrangements (Sect. 6.4). The existence of a binary before the encounter provides an evolutionary path that may agree best with the available data (see Sect. 6.5).

6.3.1. Decay of a triple system and formation of a new binary

In the simplest dynamical scenario of a triple system, we assume that Source I, which is apparently moving slower than BN, forms an eccentric massive binary, and leaves the system along with BN, as previously proposed by Rodríguez et al. (2005) and Gómez et al. (2008). In order to explain the observed velocities, we need to estimate the mass of both objects. Based on a luminosity of $2500 L_\odot$ for BN from mid-IR imaging (Gezari et al. 1998) and an ionizing photon rate of $\sim 4 \times 10^{45} s^{-1}$ from optically thin emission at $\nu = 216$ GHz (Plambeck et al. 1995), Rodríguez et al. (2005) report a mass $M_{BN} = 10 \pm 2 M_\odot$. In the following, we will assume a fiducial value of $10 M_\odot$. Constraining the mass of Source I based on an infrared or bolometric luminosity is hindered by the very high extinction toward the source (Greenhill et al.

2004b). Matthews et al. (2010) estimate a dynamical mass of $\gtrsim 7 M_\odot$ from SiO masers, whereas Reid et al. (2007) report a mass $\approx 10 M_\odot$ based on modeling of proton-electron Bremsstrahlung at 7 mm. However, from conservation of linear momentum for the BN-I system, one would estimate a mass: $M_I = 2.3 \times M_{BN} \sim 23 M_\odot$ for $M_{BN} = 10 M_\odot$. This result requires explanation of systematic errors in estimation of the dynamical mass from SiO masers by Matthews et al. (2010). We discuss implications in Sect 7.

Given mass estimates for the stars, the orbital separation of the binary can be estimated from conservation of mechanical energy. By assuming that the total kinetic energy of the system today, $\frac{1}{2}(M_I v_I^2 + M_{BN} v_{BN}^2) \sim 10^{47}$ erg, is approximately equal to the final binding energy of the binary, $(GM_{I_p} M_{I_s})/2a$, where M_{I_p} and M_{I_s} are the masses of the primary and secondary stars, respectively, and a is the binary semi-major axis, we obtain $(a/\text{AU}) = 40 m_f (1 - m_f) (M_{BN}/10 M_\odot)$, where m_f is the primary's mass fraction in the binary ($m_f = M_{I_p}/(M_{I_p} + M_{I_s})$). In the assumption of an equal-mass binary ($m_f = 0.5$), the semi-major axis is 10 AU for $M_{BN} = 10 M_\odot$, corresponding to a period of ~ 7 yr. We note that an unequal-mass binary with the same total mass would imply an even smaller orbital separation, but it would be dynamically less favorable for ejection (see discussion in following sections).

Hence, a $\sim 20 M_\odot$ equal-mass binary with a semi-major orbital axis $\lesssim 10$ AU will have a binding energy sufficient to compensate the positive kinetic energy of the BN+Source I system. Direct observation of such a tight binary may be beyond what can be achieved with current data. Size scales of 10 AU cannot be resolved with the VLA, and no maser emission has been detected with the VLBA at such small radii (resulting in the “dark band” reported by Matthews et al. 2010). However, highly eccentric orbits may be anticipated to generate local fluctuations in disk heating over just one quarter orbital period (~ 2 years), and these might be recognizable over time.

The simple analysis above allows estimation of physical parameters of the binary using basic physics (mass from linear momentum conservation and orbital sepa-

⁷ NBODY0 is a direct N-body integrator which for each particle computes the force due to all other N-1 particles. Each particle is followed with its own integration step, an essential feature when the dynamical timescales of different particles in the simulation could vary significantly.

ration from mechanical energy conservation). In order to quantify the probability of such a triple-body interaction, we simulated a system composed of three single stars of $10 M_{\odot}$ mass randomly distributed inside a sphere of 1000 AU diameter. This corresponds approximately to the area subtended by the error cones of proper motions of BN and I (Fig. 5, top panel). We ran 1000 simulations for durations of 800 years, adopting a velocity dispersion of 0.4 km s^{-1} , corresponding to a thermal velocity in a molecular cloud at $T = 10 \text{ K}$. We found that only 0.1% of configurations (1 out of 1000) gave ejections with speed higher than 25 km s^{-1} . In the case with ejection, a $10+10 M_{\odot}$ binary forms with orbital separation $\sim 7 \text{ AU}$ (Table 4). The single $10 M_{\odot}$ star is ejected with a velocity $\sim 30 \text{ km s}^{-1}$, while the massive binary leaves the interaction area with a velocity $\sim 15 \text{ km s}^{-1}$, as expected from conservation of linear momentum. These simple simulations show that the BN-I system is unlikely (probability 0.1%) to arise from chance encounters among three single stars.

6.3.2. Decay of a quadruple system and formation of a new binary

Source I and the BN object may not be the only massive objects in BN/KL. Radio source n , a YSO associated with a bipolar jet (Menten & Reid 1995) and an accretion disk (Greenhill et al. 2004b), has been proposed as a possibly significant source of luminosity in BN/KL (Menten & Reid 1995). Using MIR measurements, Greenhill et al. (2004b) estimated a luminosity of $2 \times 10^3 L_{\odot}$, corresponding to a stellar mass $\sim 8 M_{\odot}$.

Based on position measurements at 8.4 GHz, Gómez et al. (2008) proposed for source n an origin in the cluster decay along with BN and Source I. In the following, we investigate this possibility by assuming a proper motion $vx_n = -1.6 \text{ km s}^{-1}$ and $vy_n = -21.4 \text{ km s}^{-1}$, as derived by Gómez et al. (2008) at 8.4 GHz in the ONC rest-frame (but see discussion in Section 5 for arguments as to why this measurement is questionable). For $M_n = 8 M_{\odot}$ (Greenhill et al. 2004b) and $M_{\text{BN}} = 10 M_{\odot}$ (Sect. 6.3.1), conservation of linear momentum (along right ascension and declination) gives a mass $M_I \sim 8 M_{\odot}$, much lower than that estimated for the triple-system decay (Sect. 6.3.1). In this scenario, at least three YSOs (BN, I, and n) with comparable masses ($\sim 8\text{-}10 M_{\odot}$) would be running away from each other with high velocities, after a dynamical interaction occurred about 500 years ago.

However, formation of a binary is required to enable ejection of stars from a cluster. It is unlikely to be Source I because an equal-mass binary of $10 M_{\odot}$ total would not produce ionizing radiation, while a binary with very different masses for primary and secondary is an unlikely outcome for an N-body interaction (see below). Hence, in the following analysis, we assume that n is the binary. A couple of arguments support this hypothesis. First, source n has been identified as a hard X-ray source, and since a B-type star is unlikely to be active, n might be an unequal-mass binary with one low-mass member. Second, based on J and H magnitudes, Lagrange et al. (2004) stated that the SED of source n cannot be modeled as a high-mass star with a single extinction value. An additional source of IR luminosity must be added (e.g., circumstellar dust or stellar com-

panion). Although J and H band observations have not revealed bright companion IR sources with separations down to $\simeq 20 \text{ AU}$, a tighter binary remains a possibility.

In order to estimate the probability that three $\sim 10 M_{\odot}$ stars are ejected after interaction, we simulated two 4-body interactions that could generate a $10 M_{\odot}$ binary: 1) two $10 M_{\odot}$ and two $5 M_{\odot}$ stars and 2) two $10 M_{\odot}$, one $9 M_{\odot}$, and one $1 M_{\odot}$ stars. Initial conditions were set as described in Sect. 6.3.1. Among 1000 simulations, not a single event ends with ejection of a $10 M_{\odot}$ star and formation of a binary $5+5 M_{\odot}$ or $9+1 M_{\odot}$. In system 1) we observed ejections in 0.8% of cases with masses $5 M_{\odot}$ (0.7% of cases) and $10 M_{\odot}$ (0.1% of cases). The new binaries formed in those cases had total masses of $10+5 M_{\odot}$ and $10+10 M_{\odot}$ in four cases (0.4% of total) each. Orbital separations varied in the range 2-11 AU (average 9 AU) and 11-23 AU (average 14 AU), for the $10+5 M_{\odot}$ and $10+10 M_{\odot}$ binaries, respectively. In system 2) we observed ejections in 2.8% of cases but only one with mass $9 M_{\odot}$ (0.1% of cases), when a binary $10+10 M_{\odot}$ formed with an orbital separation of 10 AU (the low mass member was ejected in almost all cases). Even assuming source n was a binary before the encounter (with component masses of $5+5 M_{\odot}$ or $9+1 M_{\odot}$), an exchange interaction would eject the low-mass companion and form a quasi-equal mass binary of $\sim 15 - 20 M_{\odot}$. Hence, unless source n is about twice as luminous as believed, the star is unlikely (probability $< 0.1\%$) to be the binary that enables ejections from 4-body interaction (Table 4).

The conclusion is consistent with other pieces of evidence. Greenhill et al. (2004b) detected a disk around n with a radius $\sim 170 \text{ AU}$, larger than the separation estimated for the BN-I encounter ($50 \pm 100 \text{ AU}$), indicating that either source n did not take part in the encounter at all or that the passage occurred at large separation ($\gtrsim 200 \text{ AU}$). In this last case, source n could not have exchanged momentum/energy efficiently, making this hypothesis unlikely. In addition, Lagrange et al. (2004) report detection of a brown dwarf separated by $\sim 300 \text{ AU}$ from source n . If this is indeed a bound system, then it is unlikely to have survived an earlier dynamical interaction with BN and Source I.

We conclude that, even assuming that the 8.4 GHz proper motion measurement of source n derived by Gómez et al. (2008) is correct, source n is unlikely to have played a major role in the dynamical interaction between Source I and BN.

6.3.3. Decay of a large- N cluster

To explain the observed motion of BN with respect to Source I, Rodríguez et al. (2005) proposed an interaction among several members of a collapsing protostellar cluster. In addition to the radio sources studied here, many individual peaks of thermal IR ($7 - 24 \mu\text{m}$) emission have been identified in the BN/KL region from high angular resolution IR studies (Gezari et al. 1998; Greenhill et al. 2004b; Shuping et al. 2004). Some of these may be embedded, self-luminous protostars (Greenhill et al. 2004b; Shuping et al. 2004), suggesting a protostellar density even higher than that of the Trapezium cluster. For example, the 5 knots in IRC2 plus Source I would constitute a cluster core of $10^7 - 10^8 \text{ pc}^{-3}$ over $\sim 10^3 \text{ AU}$ within the larger ($\sim 20''$) IR cluster (Greenhill et al. 2004b). Apart

from IRc2, also IRc7 and IRc4 (and possibly IRc3) appear to be clustered around the putative expansion center within a few arcseconds (Fig. 5).

We propose that the original bound cluster may disintegrate resulting in the expansion of multiple objects with different velocities and the recoil of one (or more) of the protostars as tight binaries. This scenario would explain why the putative center of expansion is presently devoid of infrared sources (see Fig. 5). We explicitly note that, owing to the lack of astrometric IR observations, the possibility that the members of the IR cluster in BN/KL are participating in the expansion measured for Source I and BN, remains speculative.

In order to test the present scenario, we ran simulations of a protostellar cluster with eleven members, adopting masses of 0.5 (2 stars), 1 (2 stars), 2 (2 stars), 3 (1 star), 5 (1 star), and 10 (3 stars) M_{\odot} (total mass of 45 M_{\odot}), randomly distributed inside a sphere of 1000 AU diameter. The implied stellar density is 1.6×10^8 stars pc^{-3} , comparable to that found in the Orion Trapezium and the Cepheus A HW2 stellar complex (e.g. Comito et al. 2007; Jiménez-Serra et al. 2009). The choice of masses reflects plausible masses for the objects present in the region, based on radio and IR data. The three stars with 10 M_{\odot} are meant represent BN, I, and n , while the low-to-intermediate mass objects represent the IR knots associated with IRc2, IRc3, IRc4, and IRc7.

We ran 1000 simulations with durations of 800 years, adopting a velocity dispersion of 0.4 km s^{-1} . In a significant fraction of configurations (17%), stars escaped from the cluster with velocities greater than that of BN (25 km s^{-1}); we define these as runaway stars. The runaway stars had a maximum mass of 10 M_{\odot} in 0.4% of cases. High-mass runaways always required the formation of a binary with 10+5 M_{\odot} (0.2% of total cases) or 10+10 M_{\odot} total mass (0.2% of total cases). Orbital separations varied in the range 3-7 AU, with an average value of 5 AU (Table 4).

In the case that two of the massive objects in the system form a binary and source n is a high-mass YSO of 8 M_{\odot} (Greenhill et al. 2004b), the total mass of the cluster can be increased by swapping one of the 0.5 M_{\odot} stars for an 8 M_{\odot} star, keeping the same stellar density (total mass of 52.5 M_{\odot}). This would describe a system where $M_I = 10 + 10 M_{\odot}$, $M_{BN} = 10 M_{\odot}$, and $M_n = 8 M_{\odot}$. Simulations of the new system resulted in a similar number of total runaway stars (19%) of maximum 8-10 M_{\odot} in 0.7% of cases. Of these, one case out of 7 (0.1% of total) gave runaways without formation of a binary. New binaries had total masses of 10+5 M_{\odot} in one case (0.1% of total), 10+8 M_{\odot} in one case (0.1% of total), and 10+10 M_{\odot} in four cases (0.4% of total). Orbital separations varied in the range 4-11 AU, with an average value of 6.5 AU. Since results are qualitatively similar to the system with total mass of 45 M_{\odot} , we did not report the outcome of the simulations for this case in Table 4.

Our simulations show that, without the inclusion of very massive objects ($\sim 20 M_{\odot}$) in the cluster, the probability of ejecting massive members ($\geq 8 M_{\odot}$) from the system is very low ($< 1\%$). We note that previous N-body simulations from Gómez et al. (2008) resulted in a larger fraction of ejections of objects with 8 M_{\odot} (15%) because they assumed several cluster members with masses in the range 8-20 M_{\odot} and allowed for

formation of binaries as massive as 36 M_{\odot} . However, such massive objects cannot readily be identified with any of the known objects in the BN/KL region.

6.4. *Caveat with the decay of a multiple system of single stars: Implications of binary formation on the disk around Source I*

As argued from the results of N-body simulations for systems of three or more stars, Source I is likely to be a binary comprising stars of comparably high mass. The formation of a tight binary implies a close passage (O(10 AU) or less), well within the uncertainties in the analysis of proper motion data (see Sect. 5). However, the existence of disks or other structures in close proximity to BN and Source I poses a challenge to explain. We observe an ionized disk with a ~ 50 AU radius around Source I, while BN has associated dust and (molecular and ionized) gas material in a disk-like structure of tens of AU in radius (Jiang et al. 2005; Rodríguez et al. 2009). Close passages truncate disks larger in radius than the minimum stellar separation or destroy them all together. In the following, we discuss two possibilities: 1) the original disks are destroyed in the encounter and then rebuilt in the following 500 years; 2) the disks are truncated but survive the encounter.

In the first hypothesis, evidence of a disk around Source I today is indicative of a viable rebuilding mechanism fueled by either residual material dispersed from the original disks or interstellar gas in the region. We consider two possible mechanisms for rebuilding the disk: Bondi-Hoyle (B-H) accretion and tidal disruption of a low-mass object.

BH accretion is the physical mechanism through which a compact object passing through an ambient medium gains mass (Bondi & Hoyle 1944). Material within a critical radius (BH radius) becomes bound and accreted by the protostar. Equating the potential and kinetic energies, we define the BH radius $R_{BH} = GM/v^2$, an associated accretion rate $\dot{M}_{BH} = \pi\rho R_{BH}^2 v$, an accretion timescale $t_{BH} = R_{BH}/v$, and a disk mass $M_d = \dot{M}_{BH}/t_{BH}$, where M is the compact-object mass and v is the velocity relative to the surrounding medium of density ρ . Assuming $M = 20 M_{\odot}$ (Sect. 6.3) and $v = 12 \text{ km s}^{-1}$ for Source I (Sect. 3), and $n(H_2) = 10^7 \text{ cm}^{-3}$ for the molecular gas in the region (as in the hot core), we obtain: $R_{BH} = 120 \text{ AU}$, $t_{BH} = 66$ years, $\dot{M}_{BH} = 5 \times 10^{-6} M_{\odot} \text{ yr}^{-1}$, $M_d = 0.002 M_{\odot}$. Although the radius estimate is consistent with the observations, a more sophisticated modeling of BH flow, using 2D and 3D simulations for both subsonic and turbulent flows (e.g. Krumholz et al. 2005; Edgar 2004), demonstrates that gravitational focusing occurs from the initial scale of R_{BH} to the scale of an irregular accretion pseudo-disk of radius $\lesssim 0.1 \times R_{BH}$ (e.g. see Fig. 1 of Throop & Bally 2008). Hence, it appears unlikely that BH accretion would support a disk with comparable radius and symmetry to that observed. In addition, Matthews et al. (2010) report a lower-limit of $\sim 0.002 M_{\odot}$ to the disk mass, as estimated from SiO maser emission, whereas Beuther et al. (2004) report an upper limit of 0.2 M_{\odot} estimated from the continuum flux density at 345 GHz, indicating that the mass gathered in 500 years via BH would be quite low. We conclude that BH accretion can-

not explain the symmetric morphology, the size, and the mass of the disk we observe around Source I.

Another possible mechanism for building the disk around Source I is suggested by simulations from Davies et al. (2006), which show that a close encounter between $10 M_{\odot}$ and $3 M_{\odot}$ stars can lead to a tidal disruption of the low-density $3 M_{\odot}$ star and subsequent formation of a massive disk around the massive star. If, in the encounter, one low-mass star were stripped away, this process would contribute to create a massive disk/envelope around Source I, with possible rapid accretion of a significant fraction of it onto the protostar. This scenario, however, faces two major challenges. First, in order for the tidal disruption to be effective, the two stars must pass each other to within roughly one stellar radius, and by implication, the stellar density of the cluster must be quite high, $2 \times 10^9 M_{\odot} \text{ pc}^{-3}$ (Davies et al. 2006). Second, material following a disruption must be redistributed from a characteristic radius of a few tenths of an AU (orbital separation of the two stars) to the observed disk radius of tens of AU. The timescale for disk spreading by viscosity is $t_{\nu} \sim r^2/\nu$, for disk radius r and viscosity $\nu \propto \alpha$ (α is the viscosity parameter). We obtain viscous timescales ranging from 10^5 yr ($r = 10$ AU, $\alpha = 10^{-2}$) up to 10^8 yr ($r = 100$ AU, $\alpha = 10^{-3}$; Hollenbach et al. 2000). Tidal disruption is hence an improbable mechanism for the reformation of the disk around Source I in 500 years.

We conclude that the observation of a relatively large and symmetric disk around Source I is inconsistent with the formation of a binary and reformation of a circumbinary disk after 500 years.

We consider then the alternative hypothesis where the original disks survive, although severely affected by the dynamical interaction (e.g., truncation, mass redistribution, accretion burst, etc.). In order to assess conditions under which a circumstellar disk is retained in a dynamical encounter or close passage, one should include disk particles in the simulations, which is beyond the scope of this article. A follow-up paper (Moeckel et al. in prep.) will consider a dynamical interaction between a binary associated with a disk and a single star. The probability of disk survival in an interaction between a binary and a single is higher than a complex three-body interaction. The main result is that a significant fraction of the disk is retained in the case of either a clean and fast exchange of companion in the binary (one or two close passages) or in the case of survival of the binary, where the original circumbinary disk is truncated at the radius of the close passage with the single star.

6.5. (Favored) Scenario 4: Three-body interaction: BN and a pre-existing Source I binary

Ejection of massive stars and formation of tight binaries in multiple-body (≥ 3) interactions have relatively low probability ($\lesssim 1\%$) in the range of stellar densities and masses assumed in our N-body simulations (Sect. 6.3). Despite the fact that binaries are unlikely to arise by chance encounters, observations show that a large fraction ($\gtrsim 60\%$) of massive stars in OB clusters and/or associations are binary and multiple systems (Mason et al. 2009). The abundance of binaries and triples inferred from observations suggests that most stars are born that way (“primordial” binaries).

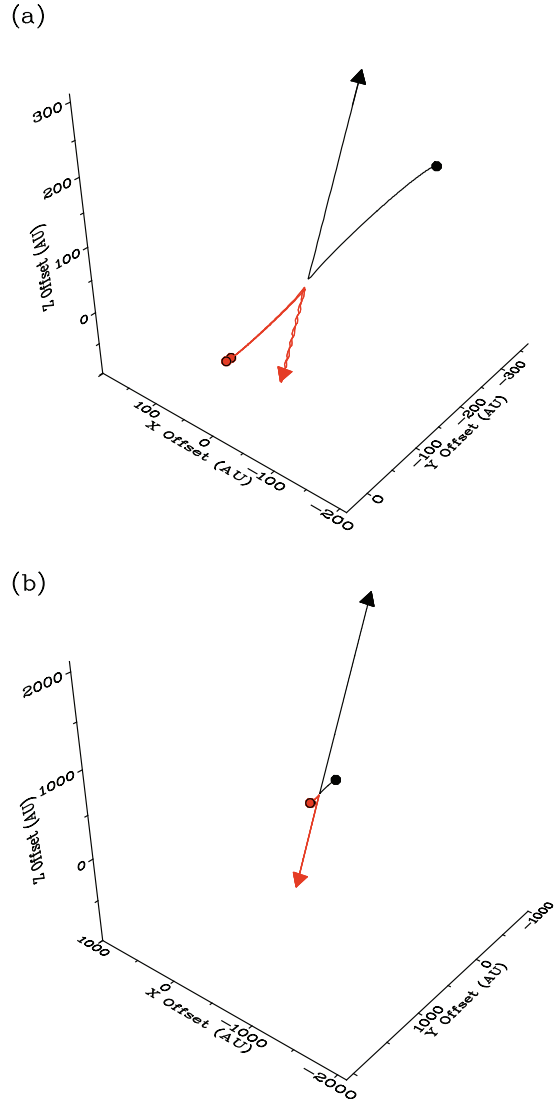


FIG. 7.— Three body simulation for the interaction between a Source I binary ($10+10 M_{\odot}$; shown in red) and BN ($10 M_{\odot}$; shown in black) at two epochs. Initial positions for the simulations are marked by filled circles, with the Source I binary components separated by 10 AU and BN at a distance of 500 AU. Initial velocities are due to the thermal velocity of the region, $v_{\text{therm}}=0.4 \text{ km s}^{-1}$. Arrows mark source positions and 3D motion directions at times after closest Source I - BN approach of (a) $t \approx 50$ years and (b) $t \approx 500$ years. After 500 years, the Source I binary and BN have positions that are ~ 3200 AU apart and are moving away from each other with 3D velocities of 14 and 29 km s^{-1} respectively, in agreement with the observations.

Combined hydrodynamic and N-body simulations have shown that primordial binaries can form from both fragmentation of collapsing cores and accretion disks (Alexander et al. 2008; Moeckel & Bate 2010).

In the following, we reconsider a 3-body interaction where two stars lie in a (primordial) binary (Source I), and a close passage occurs by the third (BN). We assume a binary of total mass $20 M_{\odot}$, with equal primary and secondary masses of $10 M_{\odot}$ and an orbital separation of 10 AU. The third star has a mass of $10 M_{\odot}$ and is at an initial distance of 500 AU. We have numerically integrated 1000 cases with three bodies in a bound system starting with a velocity dispersion

$v_{therm} = 0.4 \text{ km s}^{-1}$ and followed their dynamical interactions for 1000 years. Figure 7 shows the outcome of our simulations for one specific case. In 39% of cases, both the single and the binary stars acquire very high speeds in their interaction, flying apart in opposite directions with velocities in the range $10\text{-}90 \text{ km s}^{-1}$. In all cases, the single $10 M_{\odot}$ star runs away from the center of interaction with approximately twice the velocity of the binary, in agreement with linear momentum conservation. In the cases with ejections, the original binary survives in 15% of cases, while in 24% of cases a new binary is formed by exchanging one component (39% total). The orbital separation of binary components, averaged over the last 50 years of the simulation, varies in the range $1\text{-}9 \text{ AU}$, with an average of 4 AU . The binding energy of the tighter binary (initially at $a = 10 \text{ AU}$) compensates for the kinetic energy acquired by the two runaway stars, in agreement with conservation of mechanical energy. In the cases where the original binary survives (15%), the minimum periastron (over 1000 years) between the single and the binary varied in the range $1\text{-}60 \text{ AU}$, with an average value of 16 AU .

The new 3-body simulations show that in a high fraction of cases, massive stars are ejected (39%) and the original binary survives (15%). Stellar ejections require a massive binary ($\sim 20 M_{\odot}$) as initial condition. In exploring parameter space, we also simulated a $10 M_{\odot}$ star in parabolic orbit about a binary of total mass $11 M_{\odot}$, with mass distributed in $10+1 M_{\odot}$ or $8+3 M_{\odot}$ units. With these starting conditions, only a small fraction ($\lesssim 1\%$) resulted in ejection, and the star that was lost was the lower mass member. The process necessarily involved exchange of binary members, where the more massive companion and the third massive object formed an almost equal-mass binary whereas the lower mass member was ejected from the system. At the moment, we favor the cases where the binary survives without exchanging components, because therein the inner reaches of the accretion disk can be preserved (Sect. 6.4). A follow-up paper (Moeckel et al. in prep.) will investigate the effects of a stellar dynamical interaction on a circumbinary disk as a function of stellar mass, binary orbital separation, single-binary periastron, and swapping of binary members.

7. MASS OF SOURCE I

The assumed dynamical interaction between Source I and BN, is concomitant with an estimated mass of $\sim 20 M_{\odot}$ for Source I. Recently Matthews et al. (2010) estimated a dynamical mass using SiO maser proper motion data. This provided a lower limit of $\gtrsim 7 M_{\odot}$. The influence of non-gravitational forces on gas dynamics may be responsible for the discrepancy between dynamical masses. Matthews et al. (2010) detected both radial and rotational motions in the inferred disk around the YSO, at radii $< 100 \text{ AU}$. Although Doppler velocity data in the outflow show differential rotation of material, the actual rotation curve may be sub-Keplerian, e.g., due to radiative and/or magnetic forces, which can lead to underestimates of the central object mass. In particular, Matthews et al. (2010) reported possibly bent trajectories among proper motions and suggest that magnetic fields may play a role in shaping the gas dynamics around Source I. Girart et al. (2009) found recently that

the evolution of the gravitational collapse of a massive hot molecular core in G31.41+0.31 is controlled by magnetic fields (on scales $\sim 10000 \text{ AU}$), which appear to be effective in removing angular momentum and slowing down circumstellar gas rotation, as expected from magnetic braking (Galli et al. 2006). Shu et al. (2007) considered the case of an accretion disk threaded with magnetic fields that are squeezed in (scales $\lesssim 1000 \text{ AU}$) from the interstellar medium by gravitational collapse. They find that the poloidal component of the magnetic field produces, as a consequence of its rotation, a change in the radial force balance in the disk, giving a deviation from a Keplerian profile. The resulting rotation law has the same power-law dependence with radius as a Keplerian profile, but scaled with a coefficient $f < 1$, which includes the effects of the magnetic field. As a consequence of this deviation from Keplerian rotation, the dynamical mass of the central object derived from an observed rotation curve will be smaller than its actual value of a factor $M_{obs}/M_{true} = f^2$, where M_{true} is the true mass and M_{obs} is the observed mass. The departure from Keplerian rotation can be analytically expressed in terms of the magnetic coefficient f as: $1 - f^2 = 0.5444 M_*/(\lambda_0^2 \dot{M}_d t_{age})$ (Shu et al. 2007), where \dot{M}_d is the accretion rate onto the protostar with mass M_* , t_{age} is the stellar age, and λ_0 is a numerical coefficient from the model (assumed to be 4).⁸ Assuming for Source I $M_{true} \sim 20 M_{\odot}$ (from conservation of linear momentum of the BN-I system) and $M_{obs} \sim 8 M_{\odot}$ (from SiO maser dynamics), we derive $f^2 \sim 0.4$. Based on the formula above, this value can be readily achieved by assuming reasonable values for mass accretion rates and age: $\dot{M}_d = 10^{-5} M_{\odot} \text{ yr}^{-1}$ and $t_{age} = 10^5$ years (for $\lambda_0 = 4$). This analysis shows that, in the assumption that magnetic fields support the disk, more than half of the mass of the central object can be easily hidden from observations. Nevertheless, we caution that the estimated parameters are indicative and that careful modeling is required to determine the true mass of Source I. Future direct measurements of magnetic field amplitude in the disk around Source I, and an accurate estimate of the mass-accretion rate as well as the stellar age, will enable a better understanding of the effects of magnetic fields on mass measurement from gas dynamics.

8. WHAT IS POWERING THE WIDE-ANGLE H_2 OUTFLOW IN BN/KL?

The origin, nature, and powering source of the fast, poorly collimated bipolar outflow in BN/KL have been long debated. The H_2 finger structure consists of over 100 individual bow shocks with a large opening angle and indicates that a powerful event occurred in the center of BN/KL (e.g., Allen & Burton 1993). Proper motion studies of Herbig-Haro (HH) objects in BN/KL from the ground (Lee & Burton 2000) and with the *Hubble Space Telescope* (Doi et al. 2002) showed that more distant bullets are moving faster and indicate an origin about 1000 years ago (assuming no deceleration). Zapata et al. (2009) observed the CO(2-1) line with the Submillimeter

⁸ We note that this analysis assumes magnetic fields thread the disk and ignores the stellar magnetosphere. The formula above is then generally applicable to different kinds of stars, i.e. convective (magnetic) and radiative (non-magnetic), or, equivalently, low- and high-mass stars, respectively.

Array and identified several filaments arising from a common center and showing linear velocity gradients with distance from the center. Zapata et al. (2009) proposed that the outflow was produced by the disintegration of the young protostellar cluster formed by BN, I, and n .

We propose a similar scenario, where the dynamical interaction between BN and the Source I binary, as described in Sect. 6.5, may have produced the fast CO outflow and associated H₂ fingers in BN/KL. The outflow has a mass of about 10 M_⊙ and a kinetic energy of about 3×10^{47} ergs (Kwan & Scoville 1976). The hardening of a 20 M_⊙ binary to an orbital separation of 2 AU would release about 5×10^{47} ergs of gravitational potential energy, enough to drive the powerful outflow (3×10^{47} ergs) and compensate for the kinetic energy of the BN-I system (10^{47} erg). This outflow would not be the typical outflow powered by accretion onto a protostar, but rather the relic of a one-time event. In this picture, the expanding material was ejected at about the same time and accelerated from the area where the BN-I encounter took place, in agreement with the general “Hubble-flow” trend evidenced by proper motions of HH objects and velocity gradients in CO emission (Zapata et al. 2009). Since the disrupted circumstellar material is dispersed in all directions, this picture explains why the present structure of Source I is not related to the geometry of the outflow on large scales.

We note that, although the formation or hardening of a massive binary in a dynamical interaction can explain energetically the expansion of the outflowing gas, the physical mechanism at its origin remains unknown. More sophisticated combined N-body and hydrodynamic simulations that include also material in circumstellar disks and envelopes may help to understand the fate of circumstellar gas associated with individual protostars participating in a dynamical encounter.

9. DISCUSSION AND CONCLUSIONS

We have presented high-sensitivity, multi-epoch VLA $\lambda 7$ mm continuum observations of the radio sources in the Orion BN/KL star-forming region. These observations have shown that the radio emission from Source I is elongated NW-SE and is stable over a decade. The morphology and the stability of the emission is consistent with an ionized edge-on disk.

We measured the proper motions of Source I and the BN object for the first time at 43 GHz, confirming that they are moving with high speeds (12 and 26 km s⁻¹, respectively) approximately in opposite direction with respect to each other. We discussed possible dynamical scenarios that can explain the anomalously large motions of both BN and Source I, and implications for the dynamics of the whole BN/KL region. Our new measurements are inconsistent with a close encounter between BN and θ^1 Ori C in the past, as proposed by Tan (2004, 2008b). They confirm the previously proposed scenario of a dynamical interaction between Source I and BN 500 years ago. In particular, Gómez et al. (2008) proposed that a dynamical decay of a protostellar cluster resulted in the formation of a tight binary (Source I) and the ejection of other two sources (BN and n). However, the presence of a relatively large, massive disk around Source I and the low-probability of a multiple-body interaction among single stars, excludes that Source I formed a binary in the

course of the encounter and subsequently managed to rebuild its disk in 500 years. We propose that Source I was a binary system *before* the close passage with BN, which possibly truncated the original circumbinary disk to ~ 50 AU. Inference that this is the natal accretion disk is in agreement with disk-mediated accretion for Source I, as recently proposed by Matthews et al. (2010). This dynamical event would have resulted in the ejection of both stars and the hardening of the original binary.

The dynamical scenarios discussed in this paper were tested with N-body numerical simulations of dynamical interactions among members of a protostellar cluster. These simulations, however, illustrate a simplified physical process of gravitational interaction among point-masses. A follow-up study will include the effects of a circumbinary disk in the dynamical interactions between protostars.

The mass of Source I is still controversial. From linear momentum conservation of the BN-I system, we estimate ~ 20 M_⊙—much higher than the value estimated from SiO maser dynamics, $\gtrsim 7$ M_⊙ (Matthews et al. 2010). On one hand, a strong argument in support of the dynamical estimate is that two independent families of motions, Keplerian rotation in a disk and escape speed in an outflow, provide similar mass values, although relevant to different radii and force balance. On the other hand, the analysis in this paper is strongly based on the fact that 5 to 6 observables (proper motions, LOS velocities, and positions in the plane of the sky) are consistent with the hypothesis of a close passage between Source I and BN. One possibility for reconciling the two models is that non-gravitational forces may play a significant role in driving the dynamics of molecular gas around Source I. Assuming the disk is magnetically supported, a significant fraction of the mass of the central object can be hidden in the Keplerian velocity profile of maser emission, leading to an underestimate of the mass (Shu et al. 2007). We note that an equal-mass binary with total mass 10 M_⊙ would not produce an HII region, and an unequal-mass binary with the same total mass would have a very low-probability of surviving in a dynamical interaction with an equally-massive body (e.g., Sect. 6.5). Hence, unless we assume the presence of another very massive source in the region (e.g., n), the dynamic scenario proposed here suggests a central mass ~ 20 M_⊙ for Source I. We explicitly note that, owing to the non-linear dependence of luminosity on mass, the total luminosity developed by a binary composed of two 10 M_⊙ stars *cannot* explain the high luminosity ($\sim 10^5$ L_⊙) of the BN/KL nebula. The gravitational energy released by the hardening of a binary with total mass 20 M_⊙ would, however, be sufficient to power the gas expansion observed in H₂ and CO emission in the BN/KL nebula, although a detailed physical mechanism for such a process is still lacking.

A final, general remark concerns models of massive star formation. Source I is probably the best case known of a massive protostar with ongoing disk-mediated accretion (Matthews et al. 2010). This work shows that recent dynamical interactions played a fundamental role in shaping the protostellar properties in Orion BN/KL. Star formation in this region might be then *atypical* in the context of the classic theory of isolated low-mass star formation (Shu et al. 1987). Nevertheless, considering that most (although not all) massive stars are formed in

dense protostellar clusters (Lada & Lada 2003), dynamical interactions in very early stages of cluster evolution may be *common* in the context of crowded, massive star formation. Proper motion studies of the radio/mm continuum sources in similar regions are required to confirm this hypothesis. The EVLA, when fully commissioned, will offer broadband (up to 8 GHz) imaging, resulting in a factor of 10 improvement in continuum sensitivity, making this kind of study possible in principle for regions three times more distant. ALMA, with a similar or even better resolution, will enable similar studies at (sub)mm wavelengths. Systematic studies with these instruments

will allow us to assess the role of dynamical interactions in massive star formation.

We are grateful to Nickolas Moeckel, Mark Krumholz, Leonardo Testi, Daniele Galli, and Malcolm Walmsley for useful discussions. The data presented here were obtained under the VLA programs AM668A, AG622, AC817, and AC952. This work was supported by the National Science Foundation under Grant No. NSF AST 0507478.

APPENDIX

ABSOLUTE ASTROMETRIC ACCURACY

The absolute astrometry in each of the program datasets reported here has been determined with high accuracy (of order ~ 5 mas). The error at each epoch is taken to be the square root of the sum in quadrature of the 4 main contributions to the total error budget:

$$e_p = \sqrt{e_t^2 + e_n^2 + e_s^2 + e_\nu^2}$$

where individual contributions account for angular separation (calibrator to target), noise limited or fitting uncertainty, source structure, and frequency-dependent errors. Below we describe in detail individual error contributions:

- e_t is the theoretical error in computing the absolute astrometry from a calibrator with a separation of $\sim 1^\circ$ from the target. For a typical baseline length of 10 km and accuracy of 1 cm (appropriate for the VLA in A configuration), and a calibrator-target separation of 1.4° , one derives $e_t \sim 5$ mas. This is the dominant contribution to the overall error budget.
- e_n is the theoretical, noise-limited positional uncertainty, given by $e_n = 0.5 \theta / \text{SNR}$, where θ is the FWHM of the synthesized beamwidth of the array, and SNR is the peak intensity divided by the RMS noise in the map. We compared this error with the fitting error from JMFIT and took the larger of the two (typically ~ 1 mas).
- e_s is the uncertainty introduced by the source structure. Since both BN and Source I are resolved at 7 mm in A-configuration, different weighting schemes result in slight changes in morphology, and possibly in different peak positions. We quantified this contribution by taking the dispersion (i.e., max separation) of the positions in the images with different weighting and restoring beams: $e_s \sim 1$ mas for BN and I (resolved sources) and $e_s \sim 0$ mas for H and n (point sources).
- e_ν is the error introduced by the application of the self-calibration solutions from the maser to the continuum data, having a frequency separation $\Delta\nu \sim 100 - 350$ MHz. In previous VLA experiments, we established an angular offset per MHz as large as 0.01 mas/MHz introduced by calibrating one band by another (Goddi et al. 2009). We cannot quantify this contribution for the programs described here (we observed only at one frequency offset from the $\nu = 1$ maser line), but assuming this contribution does not change much from program to program, one can anticipate a contribution at most of a few mas.

We report typical values of individual contributions in Table 2. By adding up all contributions, typical total uncertainties are ~ 5 mas.

REFERENCES

- Aarseth, S. J. 1985, Multiple time scales, p. 377 - 418, 377
 Acord, J. M., Churchwell, E., & Wood, D. O. S. 1998, ApJ, 495, L107
 Alexander, R. D., Armitage, P. J., & Cuadra, J. 2008, MNRAS, 389, 1655
 Allen, D. A., & Burton, M. G. 1993, Nature, 363, 54
 Apai, D., Bik, A., Kaper, L., Henning, T., & Zinnecker, H. 2007, ApJ, 655, 484
 Bally, J., & Zinnecker, H. 2005, AJ, 129, 2281
 Beuther, H., et al. 2004, ApJ, 616, L31
 Beuther, H., et al. 2005, ApJ, 632, 355
 Beuther, H., et al. 2006, ApJ, 636, 323
 Beuther, H., Linz, H., Bik, A., Goto, M., & Henning, T. 2010, arXiv:1001.0650
 Bondi, H., & Hoyle, F. 1944, MNRAS, 104, 273
 Bontemps, S., Andre, P., Terebey, S., & Cabrit, S. 1996, A&A, 311, 858
 Chernin, L. M., & Wright, M. C. H. 1996, ApJ, 467, 676
 Churchwell, E., Felli, M., Wood, D. O. S., & Massi, M. 1987, ApJ, 321, 516
 Comito, C., Schilke, P., Endesfelder, U., Jiménez-Serra, I., & Martín-Pintado, J. 2007, A&A, 469, 207
 Curiel, S., et al. 2006, ApJ, 638, 878
 Davies, M. B., Bate, M. R., Bonnell, I. A., Bailey, V. C., & Tout, C. A. 2006, MNRAS, 370, 2038
 Doi, T., O'Dell, C. R., & Hartigan, P. 2002, AJ, 124, 445
 Drew, J. E., Proga, D., & Stone, J. M. 1998, MNRAS, 296, L6
 Edgar, R. 2004, New Astronomy Review, 48, 843
 Galli, D., Lizano, S., Shu, F. H., & Allen, A. 2006, ApJ, 647, 374
 Garay, G., Moran, J. M., & Reid, M. J. 1987, ApJ, 314, 535
 Genzel, R., & Stutzki, J. 1989, ARA&A, 27, 41
 Getman, K. V., et al. 2005, ApJS, 160, 319
 Gezari, D. Y., Backman, D. E., & Werner, M. W. 1998, ApJ, 509, 283

- Girart, J. M., Beltrán, M. T., Zhang, Q., Rao, R., & Estalella, R. 2009, *Science*, 324, 1408
- Goddi, C., Greenhill, L. J., Chandler, C. J., Humphreys, E. M. L., Matthews, L. D., & Gray, M. D. 2009, *ApJ*, 698, 1165
- Gómez, L., Rodríguez, L. F., Loinard, L., Lizano, S., Poveda, A., & Allen, C. 2005, *ApJ*, 635, 1166
- Gómez, L., Rodríguez, L. F., Loinard, L., Lizano, S., Allen, C., Poveda, A., & Menten, K. M. 2008, *ApJ*, 685, 333
- Goodman, J., & Hut, P. 1993, *ApJ*, 403, 271
- Greenhill, L. J., Gwinn, C. R., Schwartz, C., Moran, J. M., & Diamond, P. J. 1998, *Nature*, 396, 650
- Greenhill, L. J., Reid, M. J., Chandler, C. J., Diamond, P. J., & Elitzur, M. 2004a, *Star Formation at High Angular Resolution*, 221, 155
- Greenhill, L. J., Gezari, D. Y., Danchi, W. C., Najita, J., Monnier, J. D., & Tuthill, P. G. 2004b, *ApJ*, 605, L57
- Hillenbrand, L. A. 1997, *AJ*, 113, 1733
- Hollenbach, D. J., Yorke, H. W., & Johnstone, D. 2000, *Protostars and Planets IV*, 401
- Hoare, M. G. 2006, *ApJ*, 649, 856
- Jiang, Z., Tamura, M., Fukagawa, M., Hough, J., Lucas, P., Suto, H., Ishii, M., & Yang, J. 2005, *Nature*, 437, 112
- Jiménez-Serra, I., Martín-Pintado, J., Caselli, P., Martín, S., Rodríguez-Franco, A., Chandler, C., & Winters, J. M. 2009, *ApJ*, 703, L157
- Keto, E. 2003, *ApJ*, 599, 1196
- Keto, E. 2007, *ApJ*, 666, 976
- Kim, M. K., et al. 2008, *PASJ*, 60, 991
- Königl, A., & Pudritz, R. E. 2000, *Protostars and Planets IV*, 75
- Kraus, S., et al. 2007, *A&A*, 466, 649
- Kroupa, P. 1995, *MNRAS*, 277, 1491
- Krumholz, M. R., McKee, C. F., & Klein, R. I. 2005, *ApJ*, 618, 757
- Kwan, J., & Scoville, N. 1976, *ApJ*, 210, L39
- Lada, C. J., & Lada, E. A. 2003, *ARA&A*, 41, 57
- Lagrange, A.-M., et al. 2004, *A&A*, 417, L11
- Lee, J.-K., & Burton, M. G. 2000, *MNRAS*, 315, 11
- Lonsdale, C. J., Becklin, E. E., Lee, T. J., & Stewart, J. M. 1982, *AJ*, 87, 1819
- Marti, J., Rodríguez, L. F., & Reipurth, B. 1995, *ApJ*, 449, 184
- Mason, B. D., Hartkopf, W. I., Gies, D. R., Henry, T. J., & Helsel, J. W. 2009, *AJ*, 137, 3358
- Matthews, L. D., Greenhill, L. J., Goddi, C., Chandler, C. J., Humphreys, E. M. L., & Kunz, M. W. 2010, *ApJ*, 708, 80
- Menten, K. M., & Reid, M. J. 1995, *ApJ*, 445, L157
- Menten, K. M., Reid, M. J., Forbrich, J., & Brunthaler, A. 2007, *A&A*, 474, 515
- Moeckel, N., & Bally, J. 2006, *ApJ*, 653, 437
- Moeckel, N., & Bally, J. 2007, *ApJ*, 661, L183
- Moeckel, N., & Throop, H. B. 2009, *ApJ*, 707, 268
- Moeckel, N., & Bate, M. R. 2010, *MNRAS*, 274
- Monin, J.-L., Clarke, C. J., Prato, L., & McCabe, C. 2007, *Protostars and Planets V*, 395
- Ostriker, E. C. 1994, *ApJ*, 424, 292
- Panagia, N., & Felli, M. 1975, *A&A*, 39, 1
- Pfalzner, S. 2006, *ApJ*, 652, L129
- Plambeck, R. L., Wright, M. C. H., Mundy, L. G., & Looney, L. W. 1995, *ApJ*, 455, L189
- Preibisch, T., Balega, Y., Hofmann, K.-H., Weigelt, G., & Zinnecker, H. 1999, *New Astronomy*, 4, 531
- Reid, M. J., Menten, K. M., Greenhill, L. J., & Chandler, C. J. 2007, *ApJ*, 664, 950
- Reipurth, B. 2000, *AJ*, 120, 3177
- Reynolds, R. J. 1986, *AJ*, 92, 653
- Rodríguez, L. F., Delgado-Arellano, V. G., Gómez, Y., Reipurth, B., Torrelles, J. M., Noriega-Crespo, A., Raga, A. C., & Cantó, J. 2000, *AJ*, 119, 8
- Rodríguez, L. F., Poveda, A., Lizano, S., & Allen, C. 2005, *ApJ*, 627, L65
- Rodríguez, L. F., Zapata, L. A., & Ho, P. T. P. 2009, *ApJ*, 692, 162
- Scoville, N., Kleinmann, S. G., Hall, D. N. B., & Ridgway, S. T. 1983, *ApJ*, 275, 201
- Shu, F. H., Adams, F. C., & Lizano, S. 1987, *ARA&A*, 25, 23
- Shu, F. H., Najita, J. R., Shang, H., & Li, Z.-Y. 2000, *Protostars and Planets IV*, 789
- Shu, F. H., Galli, D., Lizano, S., Glassgold, A. E., & Diamond, P. H. 2007, *ApJ*, 665, 535
- Shuping, R. Y., Morris, M., & Bally, J. 2004, *AJ*, 128, 363
- Stahler, S. W., & Palla, F. 2005, *The Formation of Stars*, by Steven W. Stahler, Francesco Palla, pp. 865. ISBN 3-527-40559-3. Wiley-VCH
- Stahl, O., Wade, G., Petit, V., Stober, B., & Schanne, L. 2008, *A&A*, 487, 323
- Tan, J. C. 2004, *ApJ*, 607, L47
- Tan, J. C. 2008a, *Massive Star Formation: Observations Confront Theory*, 387, 346
- Tan, J. C. 2008b, arXiv:0807.3771
- Throop, H. B., & Bally, J. 2008, *AJ*, 135, 2380
- van Altena, W. F., Lee, J. T., Lee, J.-F., Lu, P. K., & Usgren, A. R. 1988, *AJ*, 95, 1744
- Wright, M. C. H., Plambeck, R. L., Mundy, L. G., & Looney, L. W. 1995, *ApJ*, 455, L185
- Zapata, L. A., Schmid-Burgk, J., Ho, P. T. P., Rodríguez, L. F., & Menten, K. M. 2009, *ApJ*, 704, L45
- Zinnecker, H., & Yorke, H. W. 2007, *ARA&A*, 45, 481